



# Recycling polyamide 6 fishing nets and carbon fibers for the development of novel sustainable composites: Properties and LCA process analysis

Francesco Pasciucco <sup>a</sup> , Damiano Rossi <sup>b,\*</sup> , Emanuele Maccaferri <sup>c</sup> , Isabella Pecorini <sup>a</sup> ,  
Loris Giorgini <sup>c</sup>, Maurizia Seggiani <sup>b</sup> 

<sup>a</sup> Department of Engineering for Energy, Systems, Territory and Constructions, University of Pisa, Via Carlo Francesco Gabba 22, 56122, Pisa, Italy

<sup>b</sup> Department of Civil and Industrial Engineering, University of Pisa, Largo Lucio Lazzarino 1, 56122, Pisa, Italy

<sup>c</sup> Department of Industrial Chemistry "Toso Montanari", University of Bologna, Viale del Risorgimento 4, Bologna, 40136, Italy

## ARTICLE INFO

Handling editor: Panos Seferlis

### Keywords:

Fishing nets  
Polyamide 6  
Carbon fibers  
Recycling  
Life cycle assessment  
LCA

## ABSTRACT

Fishing nets and related gear account for approximately 20% of the total plastic waste in the ocean, amounting to around 640,000 tons per year. Efforts are underway to develop circular economy strategies for the reuse and recycling of marine plastics. In this context, the present study introduces an innovative approach for developing advanced composite materials, employing recycled polyamide 6 (rPA6) derived from fishing nets and reinforced with recycled carbon fibers (rCF) recovered from epoxy resins through a novel thermo-oxidative process. The process involves pyrolysis at 510 °C in nitrogen to degrade the epoxy matrix, followed by gasification in air to produce clean rCF with enhanced adhesion to rPA6, eliminating the need for new sizing. This treatment increases the presence of polar groups on the surface of rCF compared to virgin carbon fibers (vCF), improving the O/C ratio (from 0.021 to 0.054 wt%) while maintaining their dimensions (7–8 μm) and surface smoothness, resulting in similar mechanical properties (293 ± 20 versus 282 ± 35 GPa). The improved compatibility of rCF with rPA6, compared to vCF, is demonstrated by the enhanced tensile modulus (11.1 and 13.1 GPa) and impact toughness (25.9 and 28.4 kJ/m<sup>2</sup>) observed in vCF/rPA6 and rCF/rPA6 composites, respectively, at the highest fiber loading of 15 wt%, in contrast to pure rPA6 (3.2 GPa and 11.8 kJ/m<sup>2</sup>). A Life Cycle Assessment (LCA) was conducted to evaluate the environmental sustainability of the CF-polyamide 6 composites. Three production scenarios were compared: Scenario 0 (virgin PA6 and vCF), Scenario 1 (rPA6 and vCF), and Scenario 2 (rPA6 and rCF). Scenario 2 showed the highest reduction in emissions, saving 5.74E+03 kg of CO<sub>2</sub> equivalents. While off-site wastewater treatment increased some emissions, the use of recycled materials consistently reduced the overall environmental impact, highlighting the benefits of sustainable waste recovery.

## 1. Introduction

Plastics are widely employed due to their advantageous properties and cost-efficiency, with packaging and construction sectors accounting for approximately 60% of global production. In 2022, the demand for plastics in Europe was estimated at around 57 million tons (Plastic Europe), with production rates showing significant growth. This increasing demand poses significant risks to ecosystems, particularly marine environments (Barnes et al., 2009; Peng et al., 2020; Lebreton et al., 2018), as an estimated 11 million tons of plastic waste are mismanaged and discharged into the oceans annually, a figure projected to nearly triple by 2040 (Linton et al., 2020). The improper disposal of plastic waste from marine activities is a major concern within the fishing

industry, where fishing nets and related gear contribute around 20% of the total oceanic plastic accumulation (approximately 640,000 tons/year). Furthermore, ghost fishing gear, including lost or abandoned nets, accounts for about 70% of all macroplastic debris in marine environments, highlighting the severe environmental consequences of discarded fishing equipment (Macfadyend et al., 2009; Hanke et al., 2019).

Currently, there is no specific waste recovery system or regulation for recycling plastic materials derived from marine activities; as a result, they are often landfilled or incinerated. Therefore, recycling strategies are strongly encouraged to mitigate this type of plastic waste. Despite the complexities of recycling fishing gears - due to inherent challenges in sorting, cleaning, and reprocessing durable polymers such as nylon 6, nylon 66, and HDPE (Li et al., 2016) - significant efforts are underway to

\* Corresponding author.

E-mail address: [damiano.rossi@unipi.it](mailto:damiano.rossi@unipi.it) (D. Rossi).

<https://doi.org/10.1016/j.jclepro.2024.144634>

Received 17 October 2024; Received in revised form 15 December 2024; Accepted 30 December 2024

Available online 31 December 2024

0959-6526/© 2024 The Authors. Published by Elsevier Ltd. This is an open access article under the CC BY license (<http://creativecommons.org/licenses/by/4.0/>).

promote the reuse of these plastics in new recycled products (Juan et al., 2021; Mondragon et al., 2020; Vilaplana and Karlsson, 2008). Specifically, PE and HDPE-based nets have a lower economic value, as they are primarily used to manufacture trawl nets, which are susceptible to abrasive damage and organic contamination (Basurko et al., 2023). These nets can be reprocessed with virgin HDPE through melt extrusion to preserve mechanical properties or, alternatively (Juan et al., 2021), used as fibers reinforcement in ceramic composites (Bertelsen and Ottosen, 2022; Romero-Gómez et al., 2023). For polyamide nets, thermomechanical recycling has emerged as the most promising approach, as it retains their thermal and rheological characteristics (Mondragon et al., 2020). More recently, cold-mixing techniques have been applied to produce polyamide 6-based composites from discarded nets, combined with recycled expanded polystyrene (PS) and ABS (Liotta et al., 2023).

In this context, polyamide 6, the most common polymer used in the fabrication of fishing accessories, is finding emerging applications as recycled material in various fields, including sustainable fabrics, clothing, construction and building, and more recently, within the automotive sector (Rossi et al., 2024). This latter opportunity is increasingly being leveraged by some prestigious automotive companies which, driven by the new End-of-Life regulation in the production of new vehicles (End-of-Life Vehicles Available online), have patented car components (Econyl® and Circulen-Recover®) made from nylon recovered from maritime plastics (CirculenRecover Available online, ECONYL Available online).

Polymer materials can be reinforced with Carbon Fibers (CF) to produce Carbon Fibers Reinforced Polymers (CFRP) with enhanced high strength, stiffness, low density, and corrosion resistance. These advanced materials are used in aerospace, wind turbine blades, sports and leisure, and automotive applications (Kausar, 2019). Increasing automotive demand and the push for lightweight vehicles are driving the growth of the CF market (End-of-Life Vehicles Available online). Key factors influencing this industry segment include the need for fuel-efficient vehicles and stringent government regulations on carbon emissions. The global demand for CF reached 115,000 tons in 2023 and is projected to grow to 280,300 tons by 2030 (Lin, 2023). The world market for CF in the automotive industry was estimated at 7000 tonnes/year with a forecasted value of USD 10.91 billion by 2032 (Lin, 2023; Market Research Future Available online). In this context, the extensive use of CFRP is expected to lead to an increase in waste generated from manufacturing processes such as prepregs, cured composite offcuts, and end-of-life composites (Zhang et al., 2020). Incineration and landfilling are the main solutions for disposing of CFRP wastes. However, these approaches are inadequate because they cause environmental pollution and result in the loss of valuable CF (Giorgini et al., 2020). The production and cutting of CF is highly energy-intensive, consuming approximately 200–600 MJ/kg - roughly ten times more than is required for glass fibers (Meng et al., 2018). Therefore, recovering used CF can significantly reduce their potential environmental impact. Recycled carbon fibers are inherently “short” after recovery, making them ideal for reinforcing injection-moulded thermoplastics.

Thermosetting epoxy resin-based composites currently account for 75–80% of all CF-reinforced composite materials (Lebreton et al., 2018). However, recovering CF from thermoset matrices is particularly challenging due to their irreversible cross-linking, which prevents reshaping or mechanical separation. Chemical solvolysis can recover CF but requires high temperatures and prolonged aggressive reaction conditions, posing significant environmental concerns. Additionally, mechanical and chemical recycling methods often cause CF fragmentation and damage, compromising their thermal and mechanical performance in second-life recycled products (Zhang et al., 2020; Giorgini et al., 2020). Among the various recycling strategies, thermochemical degradation stands out as the most promising solution, allowing for the recovery of CF with properties similar to virgin CF, achieved with moderately low

energy consumption (Zhang et al., 2020; Giorgini et al., 2020). This process consists of two consecutive steps carried out in the temperature range of 400–600 °C. During the first pyrolysis step, the CFRP matrix decomposes in the absence of oxygen to produce syngas and condensable oil, which can help offset the energy requirement of the process itself (Meyer et al., 2009). In the second oxidative step, air is introduced to remove the char residue accumulated on the fiber surface, yielding clean fibers for reuse (Oliveux et al., 2015).

Various studies and patents are currently focused on optimizing thermo-oxidative conditions tailored to common matrices such as epoxy resins, polyesters, vinyl esters, and polyamides (Giorgini et al., 2020; Sandak et al., 2019; Wei and Hadigheh, 2024; Schwarz et al., 2020; Montorsi et al., 2022). Innovative thermal degradation approaches have demonstrated that using superheated steam (Hecker et al., 2023), CO<sub>2</sub> (Limburg et al., 2019), microwave-assisted pyrolysis (Jiang et al., 2024), and chemical acid-base pre-treatments (Wei and Hadigheh, 2023) can produce high-quality recycled CF with minimal char residue and mechanical performance similar to virgin CF. A recent pilot-scale process has been developed using a fluidized bed technique in combination with papermaking and compression moulding methods to produce recycled CFRP (Meng et al., 2017). Post-processing treatments of reclaimed CF, such as acid oxidation, plasma treatment, and gamma irradiation, enhance CF-polymer adhesion, improving CFRP mechanical properties (Tiware and Bijwe, 2014). However, achieving such conditions through a single thermal step using N<sub>2</sub> and air is considered ideal from a process perspective. In this context, thermo-oxidative processes have proven effective in increasing the surface polarity of fibers by enhancing the presence of oxygen-containing groups (e.g., C=O and -OH), making CF more compatible with polar polymer matrices such as polyamides (Tiware and Bijwe, 2014; Guo et al., 2022; Salas et al., 2023; Wang et al., 2020). Schwarz et al. (2020) recently demonstrated good compatibility between pyrolyzed CF at 560 °C and polyamide 6, although performance was slightly reduced compared to virgin fibers (Schwarz et al., 2020). A more detailed analysis by Jeantet et al. (2024) evaluated the reuse of CF with polyamide 6 matrices through pyrolytic treatment followed by thermo-oxidative steps. The study showed a 15% decrease in tensile strength compared to virgin fibers, while the elastic modulus remained unchanged (Jeantet et al., 2024). CF recycling via pyrolysis has also been successfully applied in producing CFRP filaments based on polyamide 6,6 for FDM 3D printing (Valente et al., 2023).

Considering the growing opportunity for reusing CF in polyamide matrices, the present study aims to evaluate the recycling of CF in polyamide 6 composites derived from discarded fishing nets. High-value recycled CF were obtained through an innovative thermo-oxidative process developed in previous works by Giorgini et al. (2017) (Giorgini et al., 2016) and Ciacci et al. (2022) (Ciacci et al., 2022). This was achieved by optimizing a novel semi-industrial pilot plant capable of performing both pyrolysis and the subsequent oxidation steps (pyro-gasification) within the same reactor. According to the authors (Giorgini et al., 2016; Ciacci et al., 2022), this process was found to be more sustainable, reducing CO<sub>2</sub> emissions by 40 kg CO<sub>2</sub>-eq per kg of recycled CF compared to the commercial production of virgin CF. Therefore, our objective is to integrate these two recycling streams (fishing net and CF recycling) through a comprehensive Life Cycle Assessment (LCA) to estimate the associated environmental impacts to produce recycled CF-polyamide 6 composites obtained through melt extrusion compounding. To the best of our knowledge, this type of process analysis has never been examined in the literature for the production of such CF-polyamide 6 composites. These materials find applications beyond the marine sector of fishing nets, such as in the automotive industry (Colucci et al., 2015; dos Santos et al., 2024). Consequently, they will not pose significant concerns for the marine ecosystem, as they will be managed through a specific and dedicated disposal supply chain. Furthermore, the proposed approach will contribute to the reduction of marine polyamide plastic waste, while generating commercial value through its synergic integration with CF

recycling, within the framework of circular economy.

The industrial-scale LCA study was supported by a preliminary analysis in which various samples of composite material with different virgin and recycled CF concentrations were produced through melt extrusion compounding and subsequently examined to assess their thermal, morphological, and mechanical properties in comparison to typical virgin material benchmarks. In this context, thermogravimetric analysis (TGA), differential scanning calorimetry (DSC), SEM/EDS microscopy, tensile tests, and Charpy impact testing were conducted on the various CF-polyamide 6 formulations.

## 2. Materials and methods

### 2.1. Materials

Monofilament thermoplastic polyamide 6 fishing nets were collected from the nearby port of Livorno (Italy), then subjected to washing to remove sand, sea salt, and organic residues (Fig. S17). The recycled polyamide 6 nets (rPA6) were dried overnight at room temperature and pelletised using a granulator Shini SG-3048 Chinchio Sergio (Brescia, Italy) to produce small cylindrical cuts measuring 0.5–1 mm in diameter and 2–4 mm in length.

Reclaimed CF were obtained from CFRP provided confidentially by an automotive company. Offcuts of woven long-fibers fabric of prepreg composite (epoxy matrix + T830H Torayca® CF) were selected to recover CF for incorporation in rPA6 fishing nets based on the semi-industrial pyro-gasification process previously described and optimized (Giorgini et al., 2016; Ciacci et al., 2022). This pyro-gasification process technologically involves a thermal treatment consisting of two steps. During the first one, pyrolysis, the samples are treated at 510 °C for 20 min under an inert atmosphere (N<sub>2</sub>) to thermally degrade the epoxy matrix. In the second step, gasification, the samples are subjected to an oxidizing environment (air) at 510 °C for 120 min to decompose the pyrolytic carbon (char) formed during the previous step into CO<sub>2</sub>, thus obtaining matrix-free recycled carbon fibers (rCF). This selective controlled oxidation cleaning of graphitic fibers serves to improve fiber adhesion and functionality for an enhanced chemical interaction with rPA6 without the need for the application of a new sizing. The pyrolysis and gasification steps are applied separately in this work but would be carried out as a continuous process in a large-scale plant. To reflect this, the pyrolysis and gasification steps were conducted at the same temperature (510 °C), with the residence time in each step adjusted to achieve optimal conditions for producing recycled fibers with superior overall quality.

rCF were compared against commercially available unsized virgin carbon fibers T830H Torayca® (vCF). Both rCF and vCF were manually cut to a length of 5–6 mm prior to their usage for producing PA6 composites.

### 2.2. CF-polyamide 6 composites preparation

vCF and rCF cuts were dried at 100 °C for 24 h to remove moisture. Similarly, rPA6 granules were dried for 24 h in a vacuum oven at 100 °C. The complete removal of water was assessed by monitoring the weight variation of rPA6 granules over time until a stable plateau was reached (Rossi et al., 2024). Then, mixtures of rPA6 + vCF and rPA6 + rCF with different fiber contents (5, 10, and 15 wt%) were processed using a single-screw Brabender® Extruder (GmbH & Co. KG) (Fig. S17). These blends are identified as PvCFX and PrCFX, with X representing the fiber weight percentage. The blends were produced using a consistent feed-to-head zone temperature profile of 50 | 180–200 | 240–245 | 250–255 | 240–245 °C. During processing, the screw-speed was maintained steady at 30–35 rpm, with a mean torque value ranging from 16 to 19 Nm and a mass rate of about 2 kg/h. An increase in fiber content beyond 15 wt% resulted in significantly elevated torque and extreme thermal conditions, potentially causing stress and degradation of the

polymer matrix. For this reason, a moderate fiber loading was used to maintain consistent thermal conditions and obtain comparable blends.

After extrusion, the filaments were cooled in a water bath at room temperature, and then automatically cut into pellets using a cutter Procut 3D Chinchio Sergio (Brescia, Italy). These pellets were finally dried for 24 h in a vacuum oven at 100 °C and then sealed in vacuum bags to prevent moisture absorption before conducting various characterization analyses.

### 2.3. SEM/EDS

The morphological aspects of CF-polyamide 6 composites and CF before and after pyro-gasification treatments were examined using a Quanta™ FEG 450 Scanning Electron Microscope (SEM) equipped with Energy Dispersive X-Ray Spectroscopy (EDS), manufactured by FEI Quanta ESEM Instrument (Hillsboro, US). Micrographs of the composites were taken after liquid-nitrogen brittle fracture of the surface. Prior to analysis, the sample surfaces were sputter-coated with a thin layer of gold using an Edwards Sputter Coater S150B.

### 2.4. Thermal analysis: TGA and DSC

To evaluate the thermal stability of the various composites, TGA was conducted from room temperature to 900 °C at a rate of 10 °C/min under a nitrogen flow of 20 ml/min. Subsequently, the samples were heated to 1300 °C in air at the same rate and flow. TGA analyses were performed using a NETZSCH STA 2500 Regulus Instrument (Selb, Germany). Approximately 15 mg of each sample was placed in a platinum pan to conduct the tests. All TGAs were conducted in triplicate, and average mass loss was reported.

Differential Scanning Calorimetry (DSC) was conducted on various extruded pellets to evaluate the impact of fiber addition on the PA6 degree of crystallinity. The analysis was performed using a PerkinElmer Instrument Pyris 1 DSC 6000 (Waltham, US). Approximately 20 mg of each sample was sealed in an aluminium pan and heated at a rate of 10 °C/min from –50 °C to 330 °C under a nitrogen atmosphere (50 mL/min) to remove any thermal history from processing. The samples were maintained at 250 °C for 3 min, then cooled to –50 °C at 10 °C/min, and subsequently reheated to 330 °C at 10 °C/min under the same atmosphere (50 mL/min). The melting temperature (T<sub>m</sub>) and enthalpy change (ΔH<sub>m</sub>) during the second heating phase were measured to determine the degree of crystallinity (X<sub>c</sub>) of the matrix, using the following equation:

$$X_c(\%) = \frac{\Delta H_m}{\Delta H_m^0 \cdot (1 - f_w)} \cdot 100 \quad (1)$$

where ΔH<sub>m</sub><sup>0</sup> = 240 J/g represents the melting enthalpy per gram of theoretical 100% crystalline PA6 (average between α-phase at 241 J/g and γ-phase at 239 J/g, respectively (Kato and Okamoto, 2009)). The term f<sub>w</sub> denotes the weight fraction of the fiber in the composite, rescaled on the residue at the end of thermal analysis in air atmosphere. The DSC curves presented in the article correspond to the second heating cycle. All DSC were conducted in triplicate, and average mass loss were reported.

### 2.5. Mechanical analysis

Micromechanical tensile tests were carried out on vCF and rCF to evaluate the impact of the pyro-gasification on the mechanical properties of the recycled fibers. Approximately 20–25 single fibers of 30 mm length (per sample) were tested on a universal testing machine Quasar 10 Galdabini (Varese, Italy) equipped with a 10 N load cell using a crosshead speed of 10 mm/min (ASTM D3379) (Fig. S17).

Tensile tests were performed on the produced CF-polyamide 6 composites in accordance with the UNI 527-2 standard, using type 5A dog-bone specimens. The dog-bones were obtained by injection-

moulding using a Mega Tech HD 22/50 Injection Moulding Machine Tecnica Duebi (Ancona, Italy). Pellets were initially loaded into the thermostatic barrel at 250 °C and, after 1 min, the resulting melt was mechanically injected into a stainless-steel dog-bone mould. The samples were then maintained at 80 °C for an additional minute before removal. Stress-strain tests were conducted at room temperature using a Quasar 10 Galdabini (Varese, Italy) system machine equipped with a 1 kN load cell. Each test was carried out on five replicates at a crosshead speed of 10 mm/min. Mean values and relative standard deviations were reported.

The impact properties of the composites were evaluated according to ISO179. The Charpy test was carried out on a AMSE HIT2492 machine (Torino, Italy) equipped with a 2 J Charpy pendulum. Rectangular specimens with dimension 80 × 10 × 4 mm were used. The specimens were V-notched in the middle by a V-notch type A manual cutter (notch of 45°, 2 mm deep with a 0.25 mm radius of curve at the base of notch). At least 5 specimens were tested, and an average value was reported.

## 2.6. Life-cycle-assessment

### 2.6.1. Goal and scope definition

In this study, the production of CFRP composites using rPA6 from discarded fishing nets was investigated using a Life Cycle Assessment (LCA), to evaluate the environmental sustainability of the process at an industrial level. Specifically, two alternative scenarios were modeled,

exploring the production of CFRP composites obtained through melt extrusion compounding of: i) rPA6 and vCF (Scenario 1); ii) rPA6 and rCF (Scenario 2).

LCA only assesses environmental impacts, while sustainability is a holistic concept spanning the environment, economy, and society. In view of that, Fegade and Tremblay (2017) (Fegade and Tremblay, 2017) identified 6 sustainability pointers. In addition to environmental issues, life cycle costing (LCC) and social life cycle assessment (S-LCA) methods could be applied to evaluate economic and social implications from a life cycle perspective (Parris and Kates, 2003; Jin and Xu, 2024). However, LCC and S-LCA were considered out of scope.

ISO standard 14040 and 14044 were followed for the implementation of LCA analysis. A gate-to-gate approach was adopted for system boundaries, including the consumption of materials, energy, chemicals, and transports involved in the operational phases (Fig. 1). Environmental impacts due to the construction and dismantling stages were considered out of scope and negligible compared to the manufacturing phases. System boundaries were expanded and recovered products were considered as avoided impacts, which can replace primary products (Pasciucco et al., 2023a).

Scenario 1 (rPA6 + vCF) and Scenario 2 (rPA6 + rCF) were compared with the reference scenario (Scenario 0), which is represented by the production of CFRP composites totally obtained from raw materials, i.e. through melt extrusion compounding virgin PA6 (vPA6) and vCF (vPA6 + vCF).

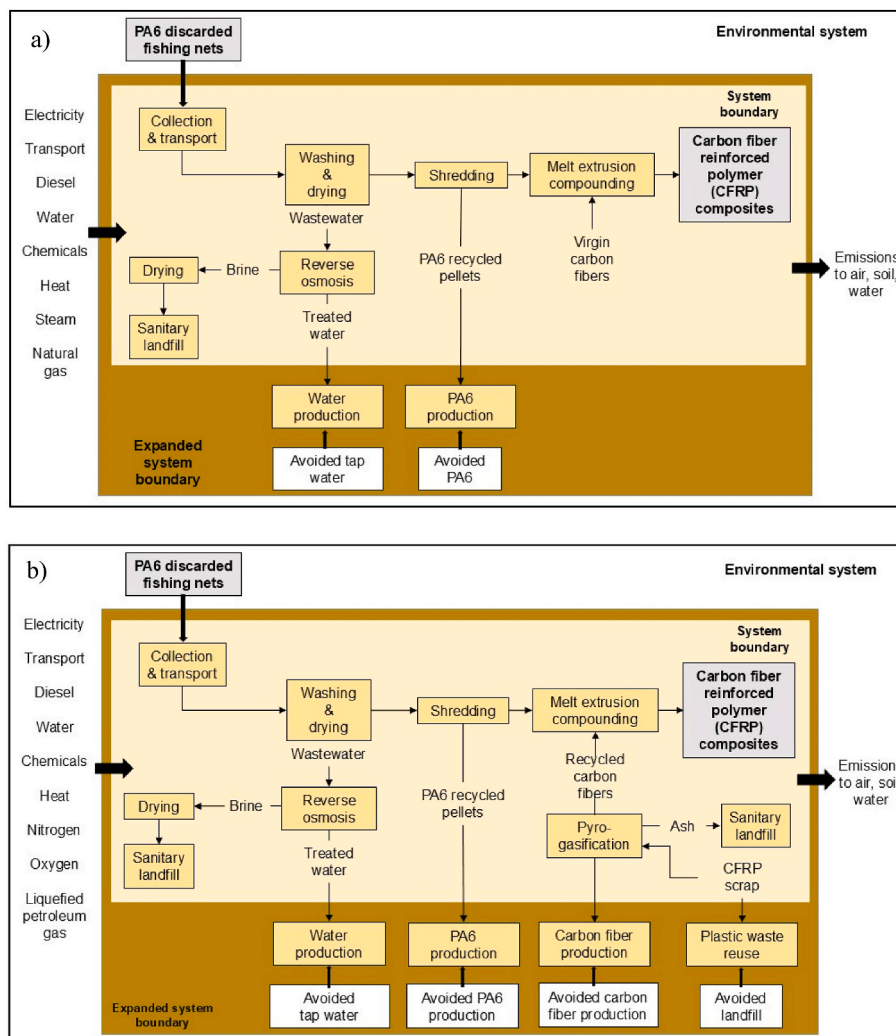


Fig. 1. System boundaries of alternative Scenario 1 (rPA6 + vCF) (a) and Scenario 2 (rPA6 and rCF) (b).

The port of Livorno was considered as a case study. Calculations and assumptions were based on an average quantity of 100 t/year of discarded fishing nets, assuming an average size of  $33 \times 3$  m and an average weight of 3.5 kg for a professional fishing net. The production of 1 ton of CFRP composites (consisting of 85 wt% PA6 and 15 wt% CF) was adopted as functional unit (FU).

### 2.6.2. Life cycle inventory analysis

Foreground data was collected from literature, experimental tests and commercial catalogues in the case of industrial machinery. Background data was retrieved from the ecoinvent database, using the latest version 3.10. Processes and phases that make up the analysed scenarios are described below. Electricity consumption of industrial machinery selected from commercial catalogues were estimated considering the power requirement and operating hours (Hospido et al., 2008).

**2.6.2.1. Recycling of PA6 from discarded fishing nets.** In the alternative scenarios (Scenario 1 and Scenario 2), the use of rPA6 from discarded fishing net to produce CFRP composites was considered.

Initially, it was assumed that discarded PA6 fishing nets are placed by fishermen in special light boxes (volume of  $120 \times 100 \times 100$  cm), distributed within the port area. By means of an electric forklift (Table S1), the boxes are loaded onto a truck and transported to the PA6 recovery plant, assuming it is in the neighbouring industrial area 6 km away. Once transported to the recovery plant, the boxes are unloaded using an electric forklift having the same technical specifications as the one previously described (Table S1), and the PA6 fishing nets are washed using a marine net washing machine to remove sand, sea salt, and organic residues. The marine net washing machine used in this study consists of a stainless-steel rotating drum (capacity volume of  $6.5 \text{ m}^3$ ) powered by an electric motor (4.5 kW, 380 VAC). According to the manufacturer's instructions, the net washing process is similar to that of a common washing machine: first, the drum is filled with tap water up to a third of the total volume; then, the remaining volume is occupied by the PA6 fishing nets, which are loaded into the marine net washing machine via a mini diesel-fueled crane (Table S2). Each wash cycle lasts 60 min and no chemical additives are added during the process.

After the washing phase, the wet fishing nets are collected using the mini crane and loaded onto the electric forklift to be transported to the nearby solar greenhouses (20 m of distance), where they are naturally dried. As showed by Kokate et al. (2014) (Kokate et al., 2014), the use solar energy for drying of PA6 has proven to be effective, removing 82% of the moisture content after 6 h of exposure. In addition, the configuration and shape of solar greenhouses significantly influence drying performance (Srinivasan and Muthukumar, 2021). In view of that, a single-span shape greenhouse oriented in an east-west direction was adopted, as Mobtaker et al. (2019) (Mobtaker et al., 2019) compared different shapes of greenhouses from the perspective of the availability of solar radiation, reporting that this configuration received approximately 8% more solar radiation during all the months in a year. To optimize the spaces inside the greenhouses, the fishing nets to be dried are fixed vertically using tie rods spaced a few centimetres apart from each other. The difference in weight of fishing nets between washing and drying phases was assumed to be negligible and no air treatment systems were foreseen, as the generation of polluting emissions was excluded.

Once dry, the fishing nets are collected and transported (via the electric forklift, Table S1) to an adjacent shed (20 m of distance) for recovery processing. Here, the fishing nets are loaded onto a conveyor belt (Table S3) feeding an industrial shredder for recycling applications (Table S4), to obtain PA6 pellets of a size suitable for subsequent treatment. At the end of the shredding phase, the PA6 pellets fall by gravity into the hopper of a screw conveyor (Table S5) feeding an industrial extruder for the final compounding with vCF (Scenario 1) or rCF (Scenario 2).

**2.6.2.2. Treatment of wastewater from fishing net washing.** Wastewater produced by fishing net washing is particularly polluted (Ozgur et al., 2023), especially in terms of chemical oxygen demand (COD) and salinity concentrations (Table S6), and need to be treated before being disposed of into the environment. Due to the expected high consumption of water, a reverse osmosis treatment was envisaged, so as to simultaneously achieve the decontamination and recovery of part of the used water (no water losses were counted in the fishing net washing phase).

The life cycle inventory (LCI) for reverse osmosis treatment was retrieved from the literature, providing the use of chemicals for disinfection of reclaimed water, pH control, membrane maintenance and coagulation-flocculation of solids. According to Qasim et al. (2019) (Qasim et al., 2019), an average recovery of 67% of the treated water was supposed, considering a reduction in COD and salinity contents by 85% and 91%, respectively (Thirugnanasambandham et al., 2016). The LCI for reverse osmosis treatment is reported in Table S7. Due to the high pollution levels and the lack of bibliographical references similar to the case studied, the LCI was filled by adopting precautionary parameters of energy consumption, chemical use, removal and recovery efficiencies.

The management of brines, which represent the remaining 33% of the flows coming out from reverse osmosis process, represents a serious environmental problem due to its high salinity. In this study, due to the uncertainties on this topic, disposal in a sanitary landfill (50 km away) was supposed for brine management (Morillo et al., 2014). In addition, a brine drying process was provided, so as to obtain a dry solid percentage of 80%, compliant with landfill disposal: according to Pasciucco et al. (2021) (Pasciucco et al., 2021), the use of a belt dryer was considered, consuming 0.8 kWh of thermal energy and 0.0375 kWh of electrical energy per kg of evaporated water.

**2.6.2.3. Recycling of CF.** The introduction of rCF was considered in Scenario 2, where the production of CFRP composites is totally made of recycled materials (rPA6 + rCF). In this study, the pyro-gasification process described in section 2.1 was considered for the production of rCF, based on the LCA study conducted by Ciacci et al. (2022) (Ciacci et al., 2022), who optimized the pyro-gasification process by investigating different operating parameters and real CFRP scrap samples. The optimal conditions found by the authors were used for process modelling as follows.

In the first part of the process, the pyrolysis step is performed: the air inside the reactor is removed by flushing  $\text{N}_2$  and the reactor is heated up to the set point temperature, which is kept constant for 20 min. After this time in pyrolysis conditions, the gasification step is carried out: throughout this phase air is blown in to oxidize the amorphous char deposited on the rCF during the pyrolysis stage. At the end of the processes, the heating is stopped, and  $\text{N}_2$  is blown again into the reactor, so as to stop the oxidation reaction and promote cooling of the system. According to the authors (Ciacci et al., 2022), the production of rCF from CFRP containing 62 wt% of T830H Torayca® CF dispersed in epoxy resin (38 wt%) showed the best environmental results, while 120 min of gasification time and a set point process temperature of  $510^\circ\text{C}$  proved to be suitable conditions to eliminate pyrolytic residues on the surface of the rCF without fiber degradation.

The ash produced during the process was supposed to be transported to a sanitary landfill (50 km away). According to the literature, the main gas outflows produced during thermal processes concern CO and  $\text{CO}_2$  emissions, and it was assumed that they were burned at temperatures above  $750^\circ\text{C}$  before being released into the atmosphere. The LCI of the pyro-gasification process and literature references are reported in Table S8.

**2.6.2.4. Production of CF and PA6 from virgin materials.** The use of vCF and vPA6 was introduced in Scenario 1 (rPA6 + vCF) and Scenario 0 (vPA6 + vCF), to highlight the impact of recycled materials in the production chain of CFRP composites.

The production of vCF was based on the study conducted by Ciacci et al. (2022) (Ciacci et al., 2022) who compared the environmental impacts from vCF and rCF productions, and the LCI provided by Meng et al. (2017) (Meng et al., 2017), as shown in Table S9. According to the authors the production of vCF was accomplished from the synthesis of polyacrylonitrile (PAN) via acrylonitrile (AN).

The appropriate ecoinvent record was used for modeling the production of vPA6, considering a production process and transport of Nylon 6 calibrated on the European market.

**2.6.2.5. Melt extrusion compounding process.** In each scenario, the production of CFRP composites is obtained through melt extrusion compounding of rPA6/vPA6 (85 wt%) and rCF/vCF (15 wt%), depending on the analysed case scenario. In this study, the environmental impacts of this process were retrieved from the ecoinvent 3.10 database, considering a co-extrusion process which includes melting of the materials, cooling and pelletizing of the final product. Previous experimental tests indicated a 2% loss relative to the input materials.

### 2.6.3. Sensitivity analysis

The treatment of wastewater produced from PA6 fishing net washing was considered a fundamental aspect, generating high environmental emissions and affected by many uncertainties. Because of that, a sensitivity analysis was conducted assuming the treatment of wastewater at an industrial wastewater treatment plant (WWTP).

Based on the analysed case study, the presence of a suitable WWTP 100 km away was considered. In addition, further distances of the WWTPs were taken into account to investigate how results change with different transport distances. The treatment of wastewater was modeled using the database provided by ecoinvent 3.10. Due to the lack of specific records in the ecoinvent database, the process was simulated considering the treatment of a wastewater stream with similar characteristics (Table S6) produced by an industrial facility. Wastewater transportation was carried out by truck.

### 2.6.4. Life cycle impact assessment

Life cycle impact assessment (LCIA) was conducted in Simapro software, using the latest version 9.6 and the CML-IA baseline method, developed by the Institute of Environmental Sciences of the Leiden University (Castagnoli et al., 2022). The CML-IA baseline is one of the most applied method in the LCA studies on plastic sector and was chosen for its compactness and ability to group the most significant environmental indicators into 11 midpoint impact categories (Marson et al., 2023).

In the LCIA, the avoided impacts due to the avoided production of commercial products were credited as emissions subtracted from the system, thus considering the advantages deriving from the replacement of conventional products (Pasciucco et al., 2023b). Specifically, the production of reclaimed water, rPA6 and rCF was assumed as avoided production of tap water, vPA6 and vCF.

Based on previous experimental results, thermal or mechanical properties of rPA6 and rCF are very close to those of virgin materials. Because of that, a replacement ratio of 1:1 was adopted. Furthermore, the use of CFRP scrap involved the avoided landfill of plastic components (Santolini et al., 2023), as disposed of landfill currently represents the main option for CFRP waste (Ciacci et al., 2022).

## 3. Results and discussion

### 3.1. CF-polyamide 6 characterization

#### 3.1.1. Thermal properties: TGA and DSC

Both vCF and rCF exhibit nearly identical degradation trends up to approximately 900 °C in N<sub>2</sub>, with T<sub>first\_onset</sub> at 902 °C (weight loss of 9 wt%) and 903 °C (weight loss of 7 wt%) for vCF and rCF, respectively

(Fig. S1). rCF exhibits a slightly higher degradation rate and leaves a lower residue at 1300 °C in air (10 wt% vs 8.5 wt%, respectively). However, such differences affect the thermal behaviour at very high temperatures, whereas in the temperature range experienced by CF during composite production and service life, the loss of thermal stability is practically negligible. The fibers further demonstrate comparable thermal stability when incorporated into the same rPA6 matrix. Consequently, PvCFX and PrCFX composites display overlapping TGA profiles, maintaining consistent thermal behaviour and stability up to approximately 380 °C (with T<sub>first\_onset</sub> ranging from 381 to 385 °C and weight loss from 7 to 8 wt%) (Fig. S2). This temperature threshold is compatible with the adopted extrusion conditions. The curves show similar sharp mass decay, reaching a plateau at 445–450 °C in N<sub>2</sub>, with residues approximately matching the original fiber concentrations in the composites (5, 10, and 15 wt%). Upon transitioning to an oxidizing environment at 1300 °C, the residues approach zero, indicating the complete combustion of both the matrix and the fibers. All composites exhibit the same thermal behaviour, regardless of the fiber loading in the matrix, which overlap with the thermogram of the recycled polyamide rPA6. This indicates a homogeneous dispersion of the fibers and good compatibility with the matrix, without any significant cracking, delamination, or debonding phenomena that could otherwise accelerate degradation processes (Adler et al., 2021; Kimura et al., 2019). Lastly, the TGA presented in Figs. S1 and S2 confirm the effective drying of rCF, vCF, and rPA6 granules, as they do not exhibit onset temperatures around 100 °C, which are typically indicative of residual water.

The DSC analyses on pellets reported in Fig. S3 confirm the weak chemical interaction between polyamide 6 and both types of CF. Moreover, no preferential induction of a specific polymorphic form is promoted by the inclusion of the CF. This is evidenced by the similar melting temperatures of the  $\alpha$  and  $\gamma$  phases of rPA6 (T<sub>m1</sub>  $\approx$  213–215 °C and T<sub>m2</sub> = 203–205 °C respectively) (Murthy, 1991; Zhang et al., 2011), as well as the glass transition temperature (T<sub>g</sub>  $\approx$  48.0–49.0 °C), all of which are confined within 1 or 2 °C difference with no particular trend observed concerning fiber loading and fiber type. This is further corroborated by the very similar degree of total crystallinity (X<sub>c</sub>  $\approx$  19.5–21.9) calculated across the various composite samples. CF could be act as nucleating agents and, due to their high conductivity, can alter the ratio between the two polymorphic forms, particularly between the interior and exterior of the composite, resulting in a skin-core morphology (Feng et al., 2013). However, these differences are usually detectable at particularly high cooling rates (up to 100 °C/min) which are higher than those employed in our study (Guglhoer et al., 2015).

#### 3.1.2. SEM/EDS morphology

The SEM images in Fig. 2a and c confirm the superior fiber cleaning performance provided by the developed thermo-oxidative pyro-gasification process (Giorgini et al., 2016; Ciacci et al., 2022), resulting in rCF having the same diameter (7–8  $\mu$ m) as the vCF, with minimal presence of char debris or impurities. In contrast, the surfaces of the fibers before the oxidative process (Fig. 2b) appear completely covered with char, rendering them unsuitable for use in composites. Interestingly, the EDS analysis reveals an almost three-fold increase in the oxygen-to-carbon (O/C wt.%) ratio on the surface of the rCF compared to the vCF (0.054  $\pm$  0.011 versus 0.021  $\pm$  0.003 wt%). This is likely due to the presence of polar groups such as hydroxyl, carbonyl, ether, and amine groups, resulting from the air oxidation treatment (Tiwari and Bijwe, 2014; Guo et al., 2022; Salas et al., 2023; Wang et al., 2020). This surface activation could not be quantified from previous thermal analysis (Section 3.1) but is evident from the SEM images of the PvCF15 and PrCF15 fractured samples (Fig. 3). These images clearly show longer segments of fiber pull-out and debonding in PvCF15 (Fig. 3a) compared to PrVC15 (Fig. 3b), indicating greater adhesion of rCF to the polyamide matrix compared to the one displayed by vCF. These findings are consistent with the recent study by Jeantet et al. (2024), which

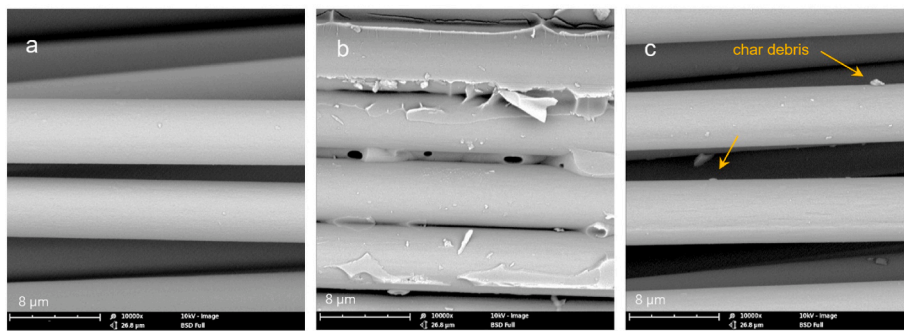


Fig. 2. SEM images of vCF (a), rCF after pyrolysis at 510 °C for 20 min in N<sub>2</sub> (b) and rCF after pyrolysis and gasification at 510 °C for 120 min in air (c).

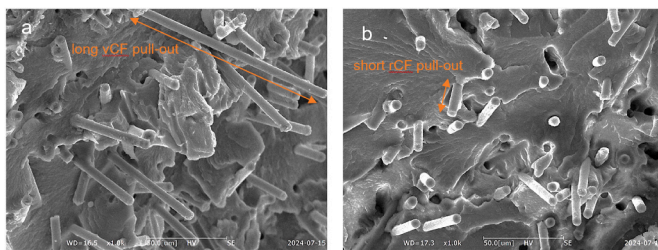


Fig. 3. SEM images of PvCF15 with major CF pull-out (a) and PrCF15 with minor CF pull-out (b).

demonstrated the effectiveness of nitrogen-air thermo-oxidative processes at temperatures around 500 °C in producing clean fibers with a high O/C ratio. This polar functionalization enhances surface energy and improves adhesion properties with PA6 (Jeantet et al., 2024).

The 5–6 mm fiber cuts initially fed into the extruder experienced fragmentation due to the mechanical stresses exerted by the screw, resulting in an average size of 100–300 μm for both types of fibers. These values represent typical dimensions for CF length in composite materials produced by melt extrusion compounding (Karsli et al., 2012).

### 3.1.3. Mechanical properties

To assess the effectiveness of the thermo-oxidative recycling process (Giorgini et al., 2016; Ciacci et al., 2022), the mechanical properties of the rCF - such as elastic modulus, stress at break, and elongation at break - were determined and found to be nearly equivalent to those of the vCF (Table 1). Note, vCF values result slightly different from those reported in the Company datasheet due to the different standards employed (TY-030B-01 versus ASTM D3379) (Toray Toray Composite Materials America). Despite the mechanical properties of the two CF being almost comparable to each other, they behave differently once embedded in the rPA6. Increasing the fiber content up to 15 wt% enhances the overall stiffness and strength of the material. Specifically, the elastic modulus increases by up to 4.1 and 3.5 times (18% raise) compared to the unloaded matrix rPA6 for rCF and vCF (Fig. 4a), respectively, while the stress at break reaches 2.7 and 2.4 times (9% raise) the values of the

Table 1  
Mechanical properties of vCF and rCF by micromechanical tensile testing.

Sample	Elastic modulus (GPa)	Stress at break (GPa)	Deformation at break (%)
vCF (T830H) <sup>a</sup>	294 ± /	5.3 ± /	1.80 ± /
vCF (T830H)	282 ± 35	5.6 ± 1.3	1.80 ± 0.20
rCF (T830H)	293 ± 20	5.8 ± 0.8	1.74 ± 0.21

<sup>a</sup> From Company datasheet based on the internal standard procedure (TY-030B-01) (Toray Toray Composite Materials America).

unloaded matrix for recycled and virgin fibers, respectively (Fig. 4b). These values are accompanied by an inevitable reduction in the material's ductility, demonstrated by a diminished strain at break of about 5.5 and 6 times (7% decrease) the value of rPA6 for vCF and rCF, respectively (Fig. 4c).

It is important to highlight that using rCF does not negatively affect the mechanical properties of the composites. Besides, rCF-reinforced composites display even slightly better performance due to improved rCF affinity with rPA6 matrix. This improvement in rCF over vCF is attributable to their oxidative surface activation (as assessed via EDS analysis) which makes rCF more compatible with the polar groups present in the polyamide 6 macromolecular backbone. The enhanced mechanical performance is further confirmed by the results of Charpy impact tests, which show an increase in the impact energy for PrCF15 and PvCF15 of 2.4 and 2.2 times (10% raise), respectively, compared to the initial values of rPA6 (Fig. 4d).

The Young's modulus and stress at break are higher than those achieved by You et al. (2021), who used 30 wt% CF treated with plasma-assisted mechanochemistry and an interlocking approach, followed by melt compounding with polyamide (You et al., 2021). Colucci et al. (2024) observed slightly superior mechanical properties compared to our findings; however, they used recycled polyamide 6,6, which offers greater tensile strength and rigidity than PA6, in addition to a higher fiber content (30 wt%) (Colucci et al., 2015). Notably, our results exceed those of Valente et al. (2023) (Valente et al., 2023) and Schwarz et al. (2020) (Schwarz et al., 2020). The authors tested single-step pyrolytic approaches to recover CF and reported reduced mechanical properties compared to vCF, specifically attributed to the lack of surface activation. The excellent compatibility between CF and PA6 observed in the present study leads to superior impact strength when compared to that achieved by dos Santos et al. (2024), who employed a simple, cost-effective method involving granulation followed by hot compression moulding of CF-PA6 waste laminates (dos Santos et al., 2024). Although direct comparisons with analogous CF-PA6 composites derived entirely from virgin materials are complex, due to the dependency of their properties on factors such as fiber length, presence of additives, fillers, molecular weight of the matrix, and stabilizers, the composites produced in this study demonstrate properties that are either comparable to or exceed those of PA6 composites with virgin fibers reported in the literature (Schwarz et al., 2020; Valente et al., 2023; Colucci et al., 2015; dos Santos et al., 2024; Xiao et al., 2023; Dinh et al., 2024). PA6 composites with 15 wt% fiber typically exhibit the following ranges: Young's modulus of 5–15 GPa, stress at break of 120–160 MPa, and impact strength of 10–25 kJ/m<sup>2</sup>.

In conclusion, the designed composites are suitable for high-performance applications where structural integrity and light-weighting are critical. The actual sustainability of the CF-polyamide 6 composites developed is evaluated in the next section, considering the best performance achieved at the highest fiber loading (15 wt%).

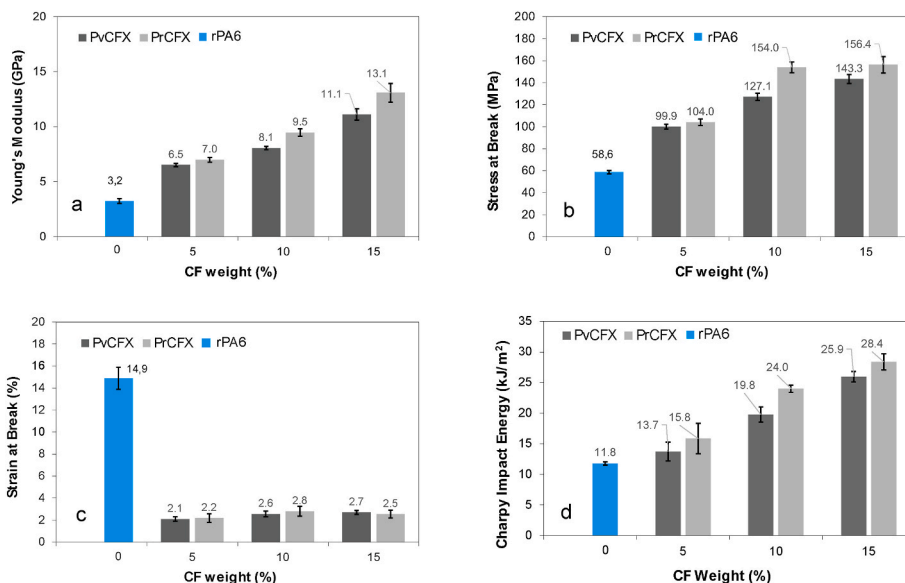


Fig. 4. Mechanical properties of rPA6, PvCFX, and PrCFX samples. Tensile tests: Young's modulus (a), stress at break (b), strain at break (c). Charpy impact energy tests (d). Mean values ± standard deviation based on 5 replicates reported on error bars.

### 3.2. LCA analysis

#### 3.2.1. General findings

An overview of the results obtained from the LCA analysis is reported in Fig. 5, displaying the percentage differences in the potential environmental impacts generated by Scenario 1 (rPA6 + vCF) Scenario 2 (rPA6 + rCF) compared to Scenario 0 (vPA6 + vCF), according to the FU. Specific values for each impact category are provided in Table S10. The negative values show that the avoided effects outweigh the direct effects (positive values) produced by the systems (Table S10).

In Scenario 1, the use of rPA6 from discarded fishing nets led to lower environmental impacts in 6 out of 11 indicators provided by the CML-IA baseline methodology, including global warming potential (GWP). Despite an overall saving in CO<sub>2</sub> emissions of 69%, the production of CFRP composites from virgin materials (Scenario 0) was still preferable in important categories such as ozone layer depletion potential (OLDP).

The melt extrusion compounding of only recycled products made

Scenario 2 the most environmentally sound option. Due to the use of both rPA6 and rCF to produce CFRP composites, the avoided impacts significantly exceeded the direct impacts generated by the system, leading to notable reductions in total emissions in 11 out of 11 environmental indicators.

As mentioned, no recovered products were applied in Scenario 0; therefore, no avoided impacts were caused. As general result, scenario comparison in Fig. 5 shows how the introduction of recycled materials into the CFRP composite production chain led to a progressive reduction in total emissions and highlights the importance of a sustainable recovery of waste products.

Contribution analyses of the several impact categories are described below. The impact categories of GWP, OLDP and eutrophication potential (EP) are described in detail, as they were identified as the environmental indicators of greatest interest for this study.

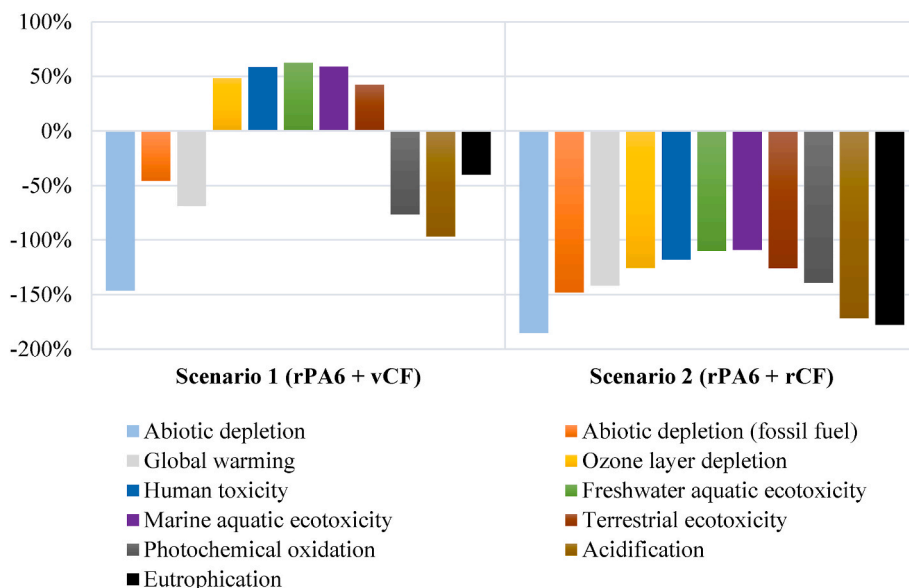


Fig. 5. Percentage differences in the environmental impacts compared to the reference (Scenario 0).



### 3.2.2. Contribution analysis to global warming potential

In GWP category, both the alternative scenarios were environmentally advantageous solutions compared to the reference, especially due to the avoided production of vPA6 (Fig. 6a).

In scenario 0, the environmental impacts generated from vPA6 production were higher than those from vCF production, representing almost 57% and 40% of CO<sub>2</sub> equivalent emissions, respectively. Total emissions were basically completed by the melt extrusion compounding process, accounting for 3% of direct impacts.

In Scenario 1, the recovery of PA6 involved significant contributions, such as the treatment of wastewater from discarded fishing net washing. Wastewater treatment, involved in the alternative scenarios for rPA6 production, resulted in the highest environmental burden (48% of direct CO<sub>2</sub> equivalent emissions), followed by vCF production (45% of direct

CO<sub>2</sub> equivalent emissions). Despite this, direct emissions in Scenario 1 (1.21E+04 kg of CO<sub>2</sub> equivalent) were similar to those in Scenario 0 (1.37E+04 kg of CO<sub>2</sub> equivalent). Indeed, Scenario 1 was freed by the production of vPA6 (accounting for an avoided impact of -7.78E+03 kg of CO<sub>2</sub> equivalent), thus showing a total release of 4.26E+03 CO<sub>2</sub> equivalent emissions (Table S10).

In Scenario 2, avoided impacts (negative values) were higher than direct effects (positive values). Wastewater treatment substantially represented the main environmental burden in Scenario 2 (77% of direct emissions). The production of rCF implied the generation of non-negligible impacts (12% of direct emissions); on the other hand, in addition to the avoided vPA6 production (59% of avoided emissions), the avoided production of vCF (41% of avoided emissions) contributed significantly, allowing an overall saving of 5.74E+03 kg of CO<sub>2</sub>

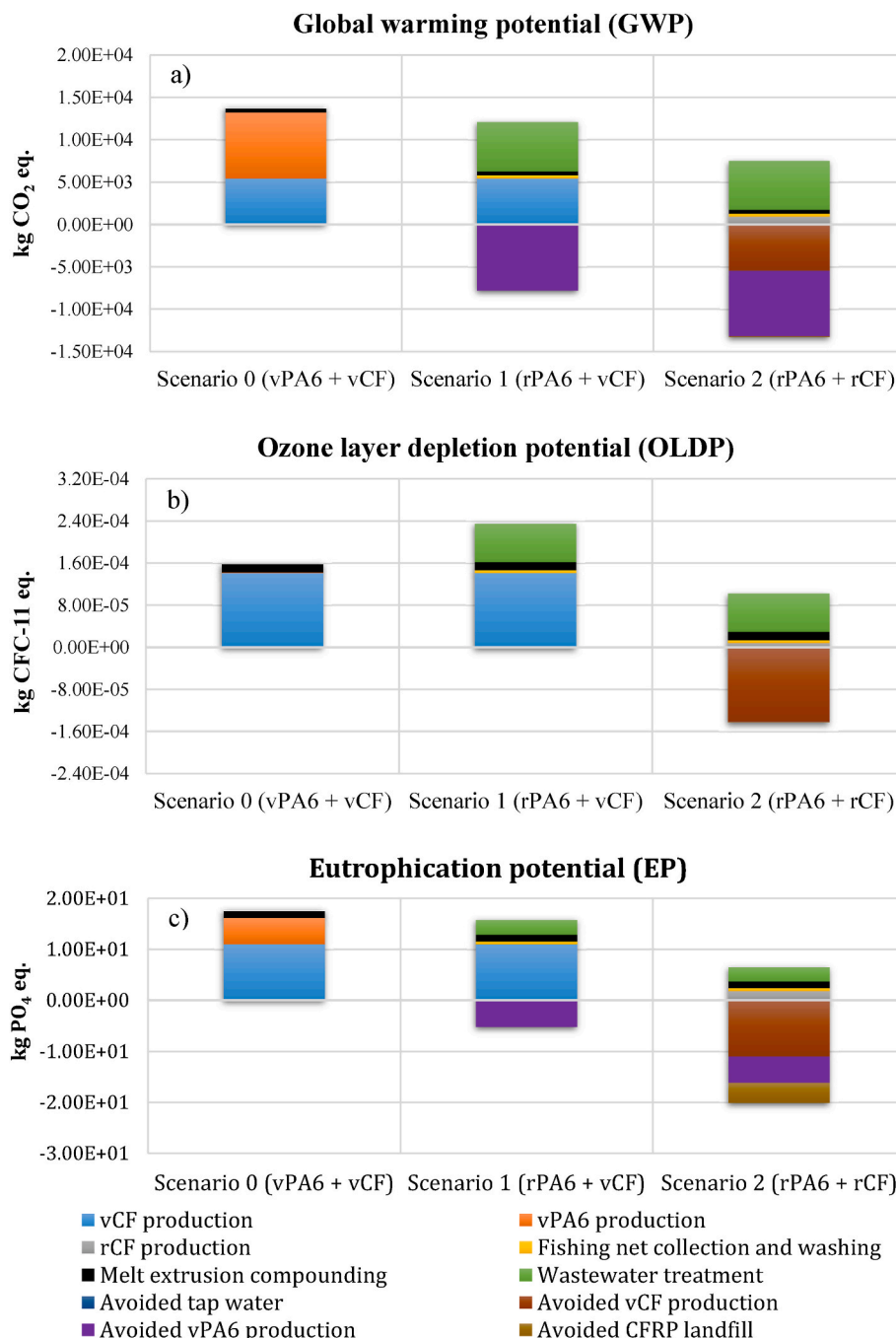


Fig. 6. Contribution analysis of GWP (a), OLDP (b) and EP (c).

equivalent emissions (Table S10).

### 3.2.3. Contribution analysis to ozone layer depletion potential

In OLDP category, Scenario 2 was the most environmentally friendly option, followed by Scenario 0 and Scenario 1, with the avoided production of vCF that played a key role (Fig. 6b).

The environmental burden due to the production of vCF accounted for almost all the impacts in Scenario 0, representing approximately 90% of CFC-11 equivalent emissions. The melt extrusion compounding process accounted for almost 10% of the total emissions, while the environmental impacts due to vPA6 production were negligible (less than 1%).

Consequently, Scenario 1 was a worse option than the reference scenario, as they showed total CFC-11 equivalent emissions of 2.33E-04 and 1.57E-04, respectively (Table S10). Indeed, in addition to the impacts deriving from vCF production (60% of direct emissions), the emissions due to the treatment of wastewater from fishing net washing (31% of direct emissions) were counted in Scenario 1; however, direct emissions were not offset by significant avoided impacts, given that the production of vPA6 had no tangible effects on this environmental indicator.

The treatment of wastewater represented the highest contribution in Scenario 2 (71% of direct impacts), accounting for 7.22E-05 kg of CFC-11 equivalent emissions. Direct emissions in Scenario 2 were lower than Scenario 0 and Scenario 1, and the avoided impacts from vCF production (99% of avoided impacts) led to a strong reduction in total emissions, showing a prevalence of avoided impacts (negative values) over direct impacts (positive values) and an overall saving of 4.04E-05 kg of CFC-11 equivalent emissions (Table S10).

### 3.2.4. Contribution analysis to eutrophication potential

In EP category, Scenario 2 was always the best option (Fig. 6c). Scenario 1 was found to be a better solution than Scenario 0, although they showed total emissions of the same order of magnitude (Table S10).

In Scenario 0, vCF production was the highest impact (63% of PO<sub>4</sub> equivalent emissions), followed by vPA6 production (almost 30%) and melt extrusion compounding process (more than 7%).

In this impact category, the treatment of wastewater from fishing net washing did not produce significant effects as in previous environmental indicators, generating 2.76E+00 kg of PO<sub>4</sub> equivalent emissions. Because of that, Scenario 1 was still affected by the huge emissions from vCF production (1.10E+01 kg of PO<sub>4</sub> equivalent, 70% of direct impacts), while the avoided production of vPA6 did not contribute significantly in terms of avoided emissions (−5.16E+00 kg of PO<sub>4</sub> equivalent emissions).

On the other hand, Scenario 2 showed an overall saving of 1.36E+01 kg of PO<sub>4</sub> equivalent emissions (Table S10). Indeed, in addition to the vPA6 avoided production, the direct emissions from system (6.50E+00 kg of PO<sub>4</sub> equivalent) were contrasted by the avoided emissions from vCF production, which was particularly influential in EP (−1.10E+01 kg of PO<sub>4</sub> equivalent). Also, the avoided CFRP landfill provided a concrete contribution (19% of avoided emissions), while it was negligible in other impact categories.

### 3.2.5. Contribution analysis to abiotic depletion and abiotic depletion (fossil fuel) potential

Contribution analysis to abiotic depletion and abiotic depletion (fossil fuel) potential are reported in Fig. S4 and Fig. S5, respectively, representing the depletion of non-renewable resources.

In abiotic depletion potential, the production of vPA6 had a huge impact on this category, accounting for 78% of the total emissions in Scenario 0. On the contrary, the recovery of rPA6 from discarded fishing nets, which was carried out both in Scenario 1 and Scenario 2, generated significant environmental benefits due to the avoided vPA6 production. The production of vCF and wastewater treatment did not particularly affect abiotic depletion potential; therefore, both Scenario 1 and

Scenario 2 showed a predominance of the avoided impacts (negative values), allowing for an overall saving of 3.28E-02 and 6.04E-02 kg of Sb equivalent, respectively (Table S10).

On the other hand, both vCF and vPA6 productions provided important contributions in abiotic depletion (fossil fuel) potential, accounting for 53% and 45% of total emissions in Scenario 0. At the same time, wastewater treatment produced a notable impact 8.46E+04 MJ in this category, representing 42% and 84% of direct emissions in Scenario 1 and Scenario 2, respectively. Because of that, both Scenario 1 and Scenario 2 were better configuration than the reference thanks to the avoided emissions from vCF and vPA6 productions. Anyway, the avoided effects outweighed the direct effects only in Scenario 2, showing a total saving of 9.77E+04 MJ (Table S10).

### 3.2.6. Contribution analysis to human toxicity, freshwater aquatic ecotoxicity, marine aquatic ecotoxicity and terrestrial ecotoxicity potential

Contribution analyses to human toxicity (Fig. S6), freshwater aquatic ecotoxicity (Fig. S7), marine aquatic ecotoxicity (Fig. S8) and terrestrial ecotoxicity potential (Fig. S9) behaved similarly and were strongly affected by the production of vCF.

Specifically, the emissions from vCF production ranged from 88% to 92% of total impacts in Scenario 0, while the production of vPA6 occupied approximately 3–5%. In addition, wastewater treatment represented a substantial contribution to direct emissions. Because of that, Scenario 0 was a better option than Scenario 1 in each ecosystem toxicity category, since the environmental credits from the avoided vPA6 production were negligible. In contrast, Scenario 2 benefited from the huge contributions of avoided vCF production and showed emission savings in each impact category (Table S10).

### 3.2.7. Contribution analysis to photochemical oxidation and acidification potential

Contribution analyses to photochemical oxidation and acidification potential are reported in Figs. S10 and S11, respectively.

The productions of vPA6 and vCF generated similar contributions in Scenario 0, accounting for 51% and 45% of the impacts in photochemical oxidation potential, 56% and 40% in acidification potential, respectively.

The emissions from wastewater treatment generated more significant contributions in photochemical oxidation potential (Fig. S10) than in acidification potential (Fig. S11); however, its contribution was not as predominant as in other indicators. For this reason, environmental credits from the avoided vPA6 production were enough to make Scenario 1 a better option than Scenario 0 in both categories.

Due to the further benefits from the avoided vCF production, Scenario 2 a prevalence of avoided impacts (negative values) over direct impacts (positive values) in acidification potential, accounting for an overall saving of 3.21E+01 kg of SO<sub>2</sub> equivalent (Table S10).

At the same time, Scenario 2 also showed overall negative emissions in photochemical oxidation potential (−8.86E-01 kg of C<sub>2</sub>H<sub>4</sub> equivalent), despite the fact that the rCF production provided a notable contribution in terms of direct emissions (6.28E-01 kg of C<sub>2</sub>H<sub>4</sub> equivalent), unlike the other impact categories.

### 3.2.8. Sensitivity analysis

In sensitivity analysis, the transport and treatment of wastewater produced from fishing net washing at an industrial WWTP was investigated.

As shown in Fig. S12, considering a distance of 100 km, the sensitivity analysis reflected the results obtained in default LCA. In fact, Scenario 2 was always the best option, while Scenario 1 showed environmental benefits compared to Scenario 0 in the same impact categories. However, it should be noted that the changes made in sensitivity analysis generally led to an increase in the environmental impacts.

Although the reverse osmosis treatment proposed in default LCA consumed a lot of chemicals and energy, and water recovery did not

provide significant benefits in terms of avoided emissions, the disposal of wastewater at an industrial WWTP generated an increase in the environmental impacts in 8 out of 11 indicators (Table 2). Specifically, this result was due by wastewater transport rather than the treatment phase at the facility, representing more than 50% of the emissions (Fig. 7).

On the other hand, the solution proposed in sensitivity analysis led to environmental benefits in important categories, such as abiotic depletion (fossil fuel) potential, GWP and OLDP, which are mainly affected by energy and chemical consumptions.

Results from sensitivity analysis suggested the quantity of wastewater to be treated and the distance from the WWTP are strategic aspects in decision planning. In view of that, further distances of the WWTPs were taken into account to investigate how results change with different transport distances.

Tables S11–S14 show the percentage differences in the environmental impacts generated by the alternative scenarios compared to default LCA, considering a WWTP distance of 50, 150, 200 and 250 km, respectively. In case of a WWTP 50 km away (Table S11), the disposal of wastewater at an industrial WWTP led to environmental benefits in 9 out of 11 indicators. Whereas, considering transport distances greater than 150 km, the on-site treatment using reverse osmosis was the preferred solution in any impact category.

Figs. S13–S16 show the percentage differences in the potential environmental impacts generated by the alternative scenarios compared to the reference (Scenario 0), considering a WWTP distance of 50, 150, 200 and 250 km, respectively. Although polluting emissions increased with the distance from the plant, scenario 2 was still the environmentally best solution in 9 out of 11 categories even considering the greater distance of 250 km (Fig. S16), confirming that the use of recycled materials has a key role in the environmental sustainability of the entire process.

### 3.3. Literature comparison on LCA

In recent years there has been a growing interest in recycled and innovative materials in polymeric matrices, including CFRP (Zheng et al., 2022), glass fibers reinforced polymers (GFRP) (Andrew and Dhakal, 2022), and geopolymer (Qaidi et al., 2022). In fact, given their excellent properties, these materials have a wide field of applicability, such as aviation (Khalil, 2017), aerospace (Al-Lami et al., 2018), automotive (Romani et al., 2023), and construction (Unis Ahmed et al., 2022) industries. In this study, the production of CFRP composites obtained through melt extrusion compounding of rPA6 from discarded fishing nets and vCF/rCF was assessed using LCA. Despite the broad interest of the scientific community, there are no similar studies in authors' knowledge, as they investigated different materials, technologies and objectives. In this context, many studies have explored the LCA of recycling CF from CFRP waste and their reprocessing in the production of composite materials using raw polymers.

**Table 2**

Percentage differences in the environmental impacts generated by the alternative scenarios in sensitivity analysis (WWTP 100 km away) compared to default LCA.

Impact category	Scenario 1	Scenario 2
Abiotic depletion [kg Sb eq.]	31%	17%
Abiotic depletion (fossil fuels) [MJ]	−27%	−30%
Global warming [kg CO <sub>2</sub> eq.]	−36%	−27%
Ozone layer depletion [kg CFC-11 eq.]	−3%	−17%
Human toxicity [kg 1,4-DB eq.]	24%	210%
Freshwater aquatic ecotoxicity [kg 1,4-DB eq.]	5%	92%
Marine aquatic ecotoxicity [kg 1,4-DB eq.]	3%	47%
Terrestrial ecotoxicity [kg 1,4-DB eq.]	73%	405%
Photochemical oxidation [kg C <sub>2</sub> H <sub>4</sub> eq.]	9%	5%
Acidification [kg SO <sub>2</sub> eq.]	94%	4%
Eutrophication [kg PO <sub>4</sub> eq.]	52%	40%

Meng et al. (2017) (Meng et al., 2018) evaluated the recovery of CF through a fluidized bed recycling process and their use in the production of CFRP considering different pathways, including compression moulding with epoxy resin and injection moulding with polypropylene. Based on the comparison with similar composite materials produced from vCF, the use of rCF resulted in lower energy consumption and a reduction of GWP by 33–51%. Karuppannan Gopalraj et al. (2021) (Karuppannan Gopalraj et al., 2021) investigated the production of CFRP through compression moulding of fresh laminating epoxy with CF recovered by a thermal recycling process, stating that thermal recycling route led to lower environmental impacts compared to conventional waste management options, such as landfill and incineration. Cheng et al. (2022) (Cheng et al., 2022) explored the recovery of CF using thermally activated oxide semiconductors (TASC) and pyrolysis technologies. Then, thermoplastic resin and rCF are remanufactured into CFRP by the resin transfer moulding (RTM) process. According to the authors, TASC performed better than pyrolysis and achieved a reduction in GWP, acidification potential and EP by 28%, 32%, and 25 %, respectively, compared to conventional disposal option. Beaucamp et al. (2024) (Beaucamp et al., 2024) tested the production of CFRP through injection moulding of lignin-based CF and polyamide 66 (PA66), predicting a reduction in GWP by 54% compared to the use of virgin materials.

On the other hand, Liotta et al. (2024) (Liotta et al., 2023) have recently tested the recycling of PA66 discarded fishing nets and the creation of composite materials in combination with recycled expanded polystyrene or poly(acrylonitrile-butadiene-styrene) matrices, observing mechanical properties similar to commercial products. Karadurmuş et al. (2024) (Karadurmuş and Bilgili, 2024) examined the LCA of synthetic fishing nets (manly composed of PA) from manufacturing to disposal, demonstrating that fishing net recycling achieved environmental benefits in all impact categories compared to incineration.

## 4. Conclusions

### 4.1. Future perspectives and challenges

The widespread adoption of the proposed recycling approach requires careful consideration and resolution of the following technical and socio-political challenges.

*LCA limitations.* Despite the differences described above, our results appear consistent with literature studies, as they highlight the positive contribution of recycled materials in the CFRP production chain, showing improved mechanical properties and environmental feasibility of the process. Potential limitations and future perspective of this work concerned the adopted system boundaries and the section of wastewater treatment. Indeed, the LCA study ends with the production of 1 ton of CFRP composites, while the use phase was excluded as it was out of scope. Although rPA6 and rCF showed improved mechanical properties, the long-term durability of the materials should be tested and included in system boundaries for a comprehensive evaluation. On the other hand, the wastewater treatment section was mainly modeled using literature data in default LCA, adopting precautionary parameters due to the existing uncertainties. Wastewater treatment through reverse osmosis generated notable environmental impacts in many indicators, and the use of chemicals contributed significantly to the production of polluting emissions. In order to maximize the environmental benefits of on-site water recovery and improve the overall sustainability of the process, the use of natural coagulants such as chitosan could be considered in a future perspective. Indeed, natural coagulants should be less harmful to the environment and have proven to be a valid alternative to conventional coagulants. However, the efficiency of the process can be affected by several factors, such as the working pH value or type of contaminants; therefore, it is advisable to test them properly before being used (Ang et al., 2016). Finally, it should be noted that

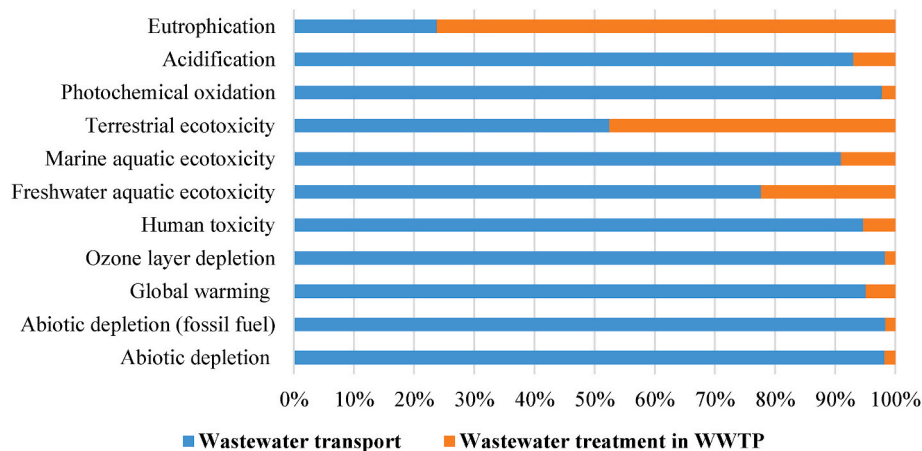


Fig. 7. Contributions to wastewater treatment in sensitivity analysis (WWTP 100 km away).

potential unpredictable challenges may arise in large-scale applications of the process. For example, despite the encouraging results of LCA, the process still requires a fair amount of energy, as well as managing the wastewater generated could prove more difficult than expected, both in practical and regulatory terms.

**Fishing Net Inhomogeneity.** Fishing nets are made from a variety of materials, including polyolefins, polyamide, and polyesters, each with distinct chemical and physical properties compared to polyamide PA6. This variability complicates recycling, as different polymers require specific temperature conditions for extrusion and may not blend effectively. Consequently, the separation of polymers in fishing gear prior to recycling is essential to ensure compatibility and maintain consistent properties in the final products. To improve adhesion and overall composite performance, the use of compatibilizing agents or process adjustments may be required, depending on the polymer matrix (Juan et al., 2021; Kozioł et al., 2022). Polyamide PA6 offers distinct advantages due to its availability and inherent compatibility with polar reclaimed carbon fibers obtained through thermo-oxidation. Conversely, polymers such as HDPE or polyolefins often necessitate fiber functionalization and surface activation (Moosburger-Will et al., 2018).

**Scaling up.** Upstream material selection is crucial for enabling large-scale composite manufacturing, ensuring consistent mechanical performance, and minimizing environmental impact. While the recovery of carbon fibers (CF) from CFRP resins is supported by well-established industrial processes, the large-scale recovery of fishing nets poses greater challenges. Effective recovery requires coordinated efforts between port authorities and the fishing industry, from managing nets during fishing operations to ensuring their collection at port facilities. Establishing efficient logistics for net collection would not only improve material separation and ensure consistent performance, but also enhance recycling rates for plastic waste. Despite the large volume of discarded nets – estimated at 640,000 tonnes of marine plastic annually (Macfadyend et al., 2009; Hanke et al., 2019), and accounting for over 70% of marine litter in the Mediterranean Sea (Liotta et al., 2023) – streamlined collection and recycling systems are crucial to address this urgent environmental challenge.

**Lack of regulations.** The European Commission (EC) has tackled the issue of End-of-Life (EOL) fishing gear and Abandoned, Lost, or otherwise Discarded Fishing Gear (ALDFG) by promoting a circular economy framework. The Single-Use Plastic (SUP) Directive (EU, 2019/904) introduced goals targeting the top 10 SUP items most commonly found on European beaches, including fishing gear (Single-Use Plastic). Current directives highlight the importance of well-structured management systems for handling EOL fishing gear, advocating for its separate collection, transport, and treatment in accordance with circular economy principles. Member States are also required to establish measurable

targets for collection and processing. In recent years, several projects and initiatives have been launched to improve marine waste management. For example, in 2020, the European Commission commissioned a study to explore ways to enhance the circularity of fishing gear (Study on Circular Design of). In the Baltic region, the MARELITT project developed strategies to identify, recover, recycle, and prevent End-of-Life fishing gear, using reverse logistics to streamline these efforts (MARELITT Project Available online). Outside Europe, the Fishing Gear Coalition developed recommendations and best practices for managing the onshore disposal of ALDFG, EOL fishing gear, and related materials in Atlantic Canada (Fishing Gear Coalition Available online). Meanwhile, the OSPAR Commission examined the barriers to recycling fishing gear in the North-East Atlantic (OSPAR Commission). While recent studies focusing on the North and South Atlantic regions demonstrate the technical feasibility of recycling networks for EOL fishing nets and identify a potential market capable of processing thousands of tons of plastic gear annually (Basurko et al., 2023; Erasmus et al., 2024), the implementation of these measures remains inconsistent. The lack of coordination and systematic regulation across regions and nations continues to undermine the effectiveness of these initiatives. In conclusion, developing an adaptable recycling system for fishing gear requires the establishment of an integrated network for collection and sorting, enabling the efficient upstream separation of materials. Strategic collaboration with fishermen and local industries, such as implementing fishing-type-specific collection schemes, can enhance sorting accuracy and facilitate material-specific recycling processes. Standardized pre-treatment protocols and modular, scalable recycling technologies are essential to accommodate regional and material variability. Additionally, leveraging advanced technologies, including artificial intelligence for automated material identification and optimized extrusion processes, can significantly improve resource management and enhance the overall efficiency of recycling systems.

#### 4.2. Potential applications

Recycled CF-PA6 composite materials could be suitable for a range of applications. Examples include the automotive sector (e.g., chassis and battery enclosures) and aerospace (e.g. body panels), where lightweight, durable, and resistant components are essential. This represents an important opportunity considering the increasingly stringent End-of-Life regulations in the production of new sustainable vehicles (End-of-Life Vehicles Available online). Other applications involve: industrial packaging for durable and reusable logistics solutions; the electronics sector for components in heat-resistant and durable devices; civil engineering for lightweight panels or structural components; sporting goods (e.g., tennis rackets and bicycles), and wind energy industry, where their high stiffness and low weight enable the design of

longer and more efficient turbine blades. Additionally, rCF/rPA6 composites could find use within the marine industry itself, enhancing the performance of boat and yacht hulls and masts while reducing the environmental impact associated with the transportation of fishing nets.

Mass production of goods and components made from recycled materials requires a reliable supply chain for the raw materials. While thermoplastic recycling is well-established, carbon fiber recycling presents greater challenges. However, industrial-scale recycling of carbon fibers via the pyro-gasification process is already feasible. This is demonstrated by the recent establishment of an Italian industrial plant operated by a major player in the environmental sector, Herambiente S.p.A. The plant was developed through a collaboration between the Industrial Chemistry Department of the University of Bologna and a technological partner, Curti S.p.A. Lavorazioni Meccaniche.

#### 4.3. Summary and key findings

This study explores the development of sustainable CFRP composites made from recycled polyamide 6 (rPA6), sourced from discarded fishing nets, reinforced with reclaimed carbon fibers (CF) obtained from a previously optimized thermo-oxidative process.

In the first part, the performance of the CFRP composites was evaluated by examining the thermal, mechanical, and morphological properties of the composites made from rPA6 reinforced with either virgin or recycled CF (vCF and rCF). The composites were produced via melt extrusion compounding at different concentrations (5, 10, and 15 wt% CF). Thermal (TGA and DSC) and morphological (SEM/EDS) analyses demonstrated the enhanced fiber-cleaning efficiency of the thermo-oxidative process, which produces rCF with the same diameter as vCF (7–8  $\mu\text{m}$ ) and minimal char residue, impurities, or defects. Interestingly, rCF exhibited both appearance and mechanical properties comparable to vCF but showed superior performance when embedded in the recycled polyamide 6. This improvement is attributed to the efficient cleaning of the fiber surface achieved through the thermo-oxidative process, which offers a dual benefit: enhancing physical adhesion between the rCF and the rPA6 matrix, and increasing surface polarity (O/C ratio from 0.021 to 0.054 wt%), thereby improving the compatibility of rCF with the polyamide 6 matrix compared to vCF. This is evidenced by the superior tensile properties (13.1 vs 11.1 GPa), and impact toughness (28.4 vs 25.9  $\text{kJ/m}^2$ ) of rCF/rPA6 composites compared vCF/rPA6 at the highest fiber loading of 15 wt%. This result can be reliably attributed to the increase in polar groups on the surface of the carbon fibers, which can interact positively with the polar groups of polyamide, enhancing the adhesion between the reinforcement and the matrix.

In the second part, the production of CFRP composites using PA6 from discarded fishing nets was studied through a Life Cycle Assessment (LCA). A gate-to-gate approach was applied to evaluate the environmental sustainability of the process at an industrial level. Two alternative scenarios were modeled, exploring the production of 1 ton of CFRP composites (consisting of 85 wt% PA6 and 15 wt% CF) obtained through melt extrusion compounding of: i) rPA6 and vCF (Scenario 1); ii) rPA6 and rCF (Scenario 2). The alternative scenarios were compared with the reference scenario (Scenario 0), which represents the production of CFRP composites through melt extrusion compounding of virgin PA6 and CF materials. A sensitivity analysis was carried out on wastewater produced from fishing net washing, considering off-site treatment at an industrial wastewater treatment plant (WWTP, assumed to be 100 km away) rather than on-site treatment using reverse osmosis. Compared to Scenario 0, Scenario 1 produced less pollutant emissions in 6 out of 11 impact categories provided by the CML-IA baseline method. Scenario 2 was the best option in all indicators due the avoided productions of vPA6 and vCF, showing a total saving of  $5.74\text{E}+03$  kg of  $\text{CO}_2$  equivalent emissions. Although off-site wastewater treatment resulted in an overall increase in pollutant emissions, except for few important categories such as global warming potential (GWP) and ozone layer depletion potential (OLDP), the sensitivity analysis confirmed that the introduction of

recycled materials into the production chain led to a progressive reduction in total emissions, highlighting the importance of a sustainable recovery of waste products.

#### 4.4. Final remarks

The main novelty of the proposed investigation lies in the ability to revalorize PA6 from end-of-life fishing nets and reclaimed carbon fiber (CF) by designing CF-PA6 composites that exhibit superior thermal and mechanical properties compared to virgin materials, as well as good processability. In the study, we examined rPA6/rCF with a 15 wt% content, though higher loadings could also be attainable. This approach not only enhances the material's properties but also promotes high circularity, making it a key strategy for repurposing a significant waste stream at the end of its life cycle.

#### CRedit authorship contribution statement

**Francesco Pasciucco:** Writing – original draft, Software, Investigation, Formal analysis, Data curation. **Damiano Rossi:** Writing – original draft, Investigation, Formal analysis, Data curation, Conceptualization. **Emanuele Maccaferri:** Visualization, Validation, Investigation, Formal analysis. **Isabella Pecorini:** Writing – review & editing, Supervision, Software, Resources. **Loris Giorgini:** Writing – review & editing, Supervision, Funding acquisition. **Maurizia Seggiani:** Writing – review & editing, Supervision, Resources, Project administration, Methodology, Funding acquisition.

#### Funding

This research was financed by the European Union - Next Generation EU (National Sustainable Mobility Centre. CN00000023. Italian Ministry of University and Research Decree n. 1033-17/06/2022. Spoke 11 - Innovative Materials & Lightweighting - Scalability Project "SUSTAINED").

#### Declaration of competing interest

The authors declare that they have no known competing financial interests or personal relationships that could have appeared to influence the work reported in this paper.

#### Acknowledgements

The authors would like to acknowledge Irene Anguillesi for her support in carrying out the thermal and mechanical tests and for her significant technical feedback and comments; Marco Sandroni for his important technical advice and great experience in processing the composite materials.

#### Appendix A. Supplementary data

Supplementary data to this article can be found online at <https://doi.org/10.1016/j.jclepro.2024.144634>.

#### Data availability

Data will be made available on request.

#### References

- Adler, S.E., Güttler, B.E., Bendler, L., Friedrich, K., 2021. Evaluation of recycled carbon fibre/epoxy composites: thermal degradation behaviour of pyrolysed and virgin carbon fibres using thermogravimetric analysis. *Adv. Ind. Eng. Polym. Res.* 4, 82–92. <https://doi.org/10.1016/j.aiepr.2021.03.003>.

- Al-Lami, A., Hilmer, P., Sinapius, M., 2018. Eco-efficiency assessment of manufacturing carbon fiber reinforced polymers (CFRP) in aerospace industry. *Aero. Sci. Technol.* 79, 669–678. <https://doi.org/10.1016/j.ast.2018.06.020>.
- Andrew, J.J., Dhakal, H.N., 2022. Sustainable biobased composites for advanced applications: recent trends and future opportunities – a critical review. *Compos. Part C Open Access* 7, 100220. <https://doi.org/10.1016/j.jcomc.2021.100220>.
- Ang, W.L., Mohammad, A.W., Benamor, A., Hilal, N., 2016. Chitosan as natural coagulant in hybrid coagulation-nanofiltration membrane process for water treatment. *J. Environ. Chem. Eng.* 4, 4857–4862. <https://doi.org/10.1016/j.jece.2016.03.029>.
- Barnes, D.K.A., Galgani, F., Thompson, R.C., Barlaz, M., 2009. Accumulation and fragmentation of plastic debris in global environments. *Philos. Trans. R. Soc. B Biol. Sci.* 364, 1985–1998. <https://doi.org/10.1098/rstb.2008.0205>.
- Basurko, O.C., Markalain, G., Mateo, M., Peña-Rodríguez, C., Mondragon, G., Larruskain, A., Larreta, J., Moalla Gil, N., 2023. End-of-Life fishing gear in Spain: quantity and recyclability. *Environ. Pollut.* 316. <https://doi.org/10.1016/j.envpol.2022.120545>.
- Beaucamp, A., Muddasar, M., Culebras, M., Collins, M.N., 2024. Sustainable lignin-based carbon fiber reinforced polymer composites: production, characterisation and life cycle analysis. *Compos. Commun.* 45, 101782. <https://doi.org/10.1016/j.coco.2023.101782>.
- Bertelsen, I.M.G., Ottosen, L.M., 2022. Recycling of waste polyethylene fishing nets as fibre reinforcement in gypsum-based materials. *Fibers Polym.* 23, 164–174. <https://doi.org/10.1007/s12221-021-9760-3>.
- Castagnoli, A., Pasciucco, F., Iannelli, R., Meoni, C., Pecorini, I., 2022. Keu contamination in tuscany: the life cycle assessment of remediation project as a decision support tool for local administration. *Sustain. Times* 14. <https://doi.org/10.3390/su142214828>.
- Cheng, H., Guo, L., Zheng, L., Qian, Z., Su, S., 2022. A closed-loop recycling process for carbon fiber-reinforced polymer waste using thermally activated oxide semiconductors: carbon fiber recycling, characterization and life cycle assessment. *Waste Manag.* 153, 283–292. <https://doi.org/10.1016/j.wasman.2022.09.008>.
- Ciacci, L., Zattini, G., Tosi, C., Berti, B., Passarini, F., Giorgini, L., 2022. Carbon fibers waste recovery via pyro-gasification: semi-industrial pilot plant testing and LCA. *Sustainability* 14, 3744. <https://doi.org/10.3390/su14073744>.
- CirculenRecover Available online: <https://www.lyondellbasell.com/en/sustainability/circulen/>.
- Colucci, G., Ostrovskaya, O., Frache, A., Martorana, B., Badini, C., 2015. The effect of mechanical recycling on the microstructure and properties of PA66 composites reinforced with carbon fibers. *J. Appl. Polym. Sci.* 132. <https://doi.org/10.1002/app.42275>.
- Dinh, D.T., Ninh, H.D., Nguyen, H.T., Nguyen, D.H., Nguyen, G.V., Nguyen, T.H., Pham, K.T., La, D.D., 2024. Polyamide 6/carbon fibre composite: an investigation of carbon fibre modifying pathways for improving mechanical properties. *Plast. Rubber Compos. Macromol. Eng.* 53, 190–199. <https://doi.org/10.1177/14658011241253553>.
- dos Santos, M.E.B., Morgado, G.F. de M., Santos, L.F., de P., Backes, E.H., Marini, J., Montagna, L.S., Passador, F.R., 2024. Mechanical recycling process: an alternative for CF/PA6 composite waste from the automotive industry. *ACS Sustain. Resour. Manag.* <https://doi.org/10.1021/acssusresmg.4c00245>.
- ECONYL Available online: <https://www.econyl.com/blog/fishing-nets-from-aquaculture-and-fish-industry-and-ghost-nets/>.
- End-of-Life Vehicles Available online: [https://environment.ec.europa.eu/topics/waste-and-recycling/end-life-vehicles\\_en](https://environment.ec.europa.eu/topics/waste-and-recycling/end-life-vehicles_en).
- Erasmus, V.N., Johannes, F.N., Amutenya, N., James, N.A., 2024. The potential contribution of end-of-life fishing nets, lines and ropes to a circular economy: the Namibian perspective. *Front. Sustain.* 5. <https://doi.org/10.3389/frsus.2024.1356265>.
- Fegade, S.L., Tremblay, J.P., 2017. Misinterpretation of green Chemistry. *Ultras. Sonochem.* 37, 686–687. <https://doi.org/10.1016/j.ulsonch.2015.04.007>.
- Feng, N., Wang, X., Wu, D., 2013. Surface modification of recycled carbon fiber and its reinforcement effect on nylon 6 composites: mechanical properties, morphology and crystallization behaviors. *Curr. Appl. Phys.* 13, 2038–2050. <https://doi.org/10.1016/j.cap.2013.09.009>.
- Fishing Gear Coalition Available online: <https://fgcac.org/>.
- Giorgini, L., Leonardi, C., Mazzocchetti, L., Zattini, G., Cavazzoni, M., Montanari, I., Tosi, C., Benelli, T., 2016. Pyrolysis of fiberglass/polyester composites: recovery and characterization of obtained products. *FME Trans.* 44, 405–414. <https://doi.org/10.5937/fmet1604405G>.
- Giorgini, L., Benelli, T., Brancolini, G., Mazzocchetti, L., 2020. Recycling of carbon fiber reinforced composite waste to close their life cycle in a cradle-to-cradle approach. *Curr. Opin. Green Sustainable Chem.* 26, 100368. <https://doi.org/10.1016/j.cogsc.2020.100368>.
- Guglhoer, T., Korkisch, M., Sause, M.G.R., 2015. Influence of carbon fibres on the crystallinity of polyamide-6. *ICCM Int. Conf. Compos. Mater.* 2015-2015-July.
- Guo, L., Xu, L., Ren, Y., Shen, Z., Fu, R., Xiao, H., Liu, J., 2022. Research on a two-step pyrolysis-oxidation process of carbon fiber-reinforced epoxy resin-based composites and analysis of product properties. *J. Environ. Chem. Eng.* 10, 107510. <https://doi.org/10.1016/j.jece.2022.107510>.
- Hanke, G., Walvoort, D., van Loon, W., Maria Addamo, A., Brosich, A., del Mar Chaves Montero, M., Eugenia Molina Jack, M., Vinci, M., Giorgetti, A., 2019. EU Marine Beach Litter Baselines.
- Hecker, M.D., Longana, M.L., Thomsen, O., Hamerton, I., 2023. Recycling of carbon fiber reinforced polymer composites with superheated steam – a review. *J. Clean. Prod.* 428, 139320. <https://doi.org/10.1016/j.jclepro.2023.139320>.
- Hospido, A., Moreira, M.T., Feijoo, G., 2008. A comparison of municipal wastewater treatment plants for big centres of population in Galicia (Spain). *Int. J. Life Cycle Assess.* 13, 57–64. <https://doi.org/10.1065/lca2007.03.314>.
- Jeantet, L., Regazzi, A., Perrin, D., Pucci, M.F., Corn, S., Quantin, J.C., Lenny, P., 2024. Recycled carbon fiber potential for reuse in carbon fiber/PA6 composite parts. *Composites, Part B* 269, 111100. <https://doi.org/10.1016/j.compositesb.2023.111100>.
- Jiang, Q., Xu, L., Ren, Y., Sun, Y., Xiao, S., Shen, Z., 2024. Carbon fiber recovery from carbon fiber reinforced polymer matrix composite by microwave pyrolysis. *Mater. Today Commun.* 40, 109462. <https://doi.org/10.1016/j.mtcomm.2024.109462>.
- Jin, B., Xu, X., 2024. Forecasts of China mainland new energy index prices through Gaussian process regressions. *J. Clean Energy Energy Storage* 1. <https://doi.org/10.1142/S2811034X24500060>.
- Juan, R., Domínguez, C., Robledo, N., Paredes, B., Galera, S., García-Muñoz, R.A., 2021. Challenges and opportunities for recycled polyethylene fishing nets: towards a circular economy. *Polymers* 13, 1–15. <https://doi.org/10.3390/polym13183155>.
- Karadurmuş, U., Bilgili, L., 2024. Environmental impacts of synthetic fishing nets from manufacturing to disposal: a case study of Türkiye in life cycle perspective. *Mar. Pollut. Bull.* 198, 115889. <https://doi.org/10.1016/j.marpolbul.2023.115889>.
- Karsli, N.G., Aytac, A., Deniz, V., 2012. Effects of initial fiber length and fiber length distribution on the properties of carbon-fiber-reinforced-polypropylene composites. *J. Reinforc. Plast. Compos.* 31, 1053–1060. <https://doi.org/10.1177/0731684412452678>.
- Karuppappan Gopalraj, S., Deviatkin, I., Horttanainen, M., Kärki, T., 2021. Life cycle assessment of a thermal recycling process as an alternative to existing CFRP and GFRP composite waste management options. *Polymers* 13, 4430. <https://doi.org/10.3390/polym13244430>.
- Katoh, Y., Okamoto, M., 2009. Crystallization controlled by layered silicates in nylon 6-clay nano-composite. *Polymer (Guildf.)* 50, 4718–4726. <https://doi.org/10.1016/j.polymer.2009.07.019>.
- Kausar, A., 2019. Advances in carbon fiber reinforced polyamide-based composite materials. *Adv. Mater. Sci.* 19, 67–82. <https://doi.org/10.2478/adms-2019-0023>.
- Khalil, Y.F., 2017. Eco-efficient lightweight carbon-fiber reinforced polymer for environmentally greener commercial aviation industry. *Sustain. Prod. Consum.* 12, 16–26. <https://doi.org/10.1016/j.spc.2017.05.004>.
- Kimura, M., Watanabe, T., Takeichi, Y., Niwa, Y., 2019. Nanoscopic origin of cracks in carbon fiber-reinforced plastic composites. *Sci. Rep.* 9, 1–9. <https://doi.org/10.1038/s41598-019-55904-2>.
- Kokate, D.H., Kale, D.M., Korpale, V.S., Shinde, Y.H., Panse, S.V., Deshmukha, S.P., Pandit, A.B., 2014. Energy conservation through solar energy assisted dryer for plastic processing industry. *Energy Proc.* 54, 376–388. <https://doi.org/10.1016/j.egypro.2014.07.281>.
- Kozioł, A., Paso, K.G., Kuciel, S., 2022. Properties and recyclability of abandoned fishing net-based plastic debris. *Catalysts* 12, 948. <https://doi.org/10.3390/catal12090948>.
- Lebreton, L., Slat, B., Ferrari, F., Sainte-Rose, B., Aitken, J., Marthouse, R., Hajbane, S., Cunsolo, S., Schwarz, A., Levivier, A., et al., 2018. Evidence that the great Pacific garbage patch is rapidly accumulating plastic. *Sci. Rep.* 8, 1–15. <https://doi.org/10.1038/s41598-018-22939-w>.
- Li, W.C., Tse, H.F., Fok, L., 2016. Plastic waste in the marine environment: a review of sources, occurrence and effects. *Sci. Total Environ.* 566–567, 333–349. <https://doi.org/10.1016/j.scitotenv.2016.05.084>.
- Limburg, M., Stockschlader, J., Quicker, P., 2019. Thermal treatment of carbon fibre reinforced polymers (Part 1: recycling). *Waste Manag. Res.* 37, 73–82. <https://doi.org/10.1177/0734242X18820251>.
- Lin, Gang, 2023. Global Carbon Fiber Composites Market Report - ATA CFT Guangzhou Co.,LTD, 2023.
- Linton, J.D., Klassen, R., Jayaraman, V., Walker, H., Brammer, S., Ruparathna, R., Hewage, K., Thomson, J., Jackson, T., Baloi, D., et al., 2020. Evaluating scenarios toward zero plastic pollution. *Science* 369, 1455–1461. <https://doi.org/10.1126/science.aba9475> (80).
- Liotta, I., Avolio, R., Castaldo, R., Gentile, G., Ambrogi, V., Errico, M.E., Cocca, M., 2023. Mitigation approach of plastic and microplastic pollution through recycling of fishing nets at the end of life. *Process Saf. Environ. Protect.* 182, 1143–1152. <https://doi.org/10.1016/j.psep.2023.12.031>.
- Macfadyen, Graeme, Huntington, Tim, Abandoned, Rod Cappell, 2009. Lost or otherwise discarded fishing gear. *FAO Fish. Aquac.* 523, 115.
- MARELITT Project Available online: <https://www.marelittbaltic.eu/>.
- Market Research Future Available online: <https://www.marketresearchfuture.com>.
- Marson, A., Piron, M., Zuliani, F., Fedele, A., Manzardo, A., 2023. Comparative life cycle assessment in the plastic sector: a systematic literature review. *Clean. Environ. Syst.* 9, 100119. <https://doi.org/10.1016/j.cesys.2023.100119>.
- Meng, F., McKechnie, J., Turner, T.A., Pickering, S.J., 2017. Energy and environmental assessment and reuse of fluidised bed recycled carbon fibres. *Compos. Part A Appl. Sci. Manuf.* 100, 206–214. <https://doi.org/10.1016/j.compositesa.2017.05.008>.
- Meng, F., Olivetti, E.A., Zhao, Y., Chang, J.C., Pickering, S.J., McKechnie, J., 2018. Comparing life cycle energy and global warming potential of carbon fiber composite recycling technologies and waste management options. *ACS Sustain. Chem. Eng.* 6, 9854–9865. <https://doi.org/10.1021/acsschemeng.8b01026>.
- Meyer, L.O., Schulte, K., Grove-Nielsen, E., 2009. CFRP-recycling following a pyrolysis route: process optimization and potentials. *J. Compos. Mater.* 43, 1121–1132. <https://doi.org/10.1177/0021998308097737>.
- Mobtaker, H.G., Ajabshirchi, Y., Ranjbar, S.F., Matloobi, M., 2019. Simulation of thermal performance of solar greenhouse in north-west of Iran: an experimental validation. *Renew. Energy* 135, 88–97. <https://doi.org/10.1016/j.renene.2018.10.003>.

- Mondragon, G., Kortaberria, G., Mendiburu, E., González, N., Arbelaz, A., Peña-Rodríguez, C., 2020. Thermomechanical recycling of polyamide 6 from fishing nets waste. *J. Appl. Polym. Sci.* 137, 1–6. <https://doi.org/10.1002/app.48442>.
- Montorsi, F., Brancolini, G., Mazzocchetti, L., Benelli, T., Giorgini, L., 2022. Optimization of pyro-gasification of carbon fiber reinforced polymers (CFRPs). *Macromol. Symp.* 405, 1–4. <https://doi.org/10.1002/masy.202100384>.
- Moosburger-Will, J., Bauer, M., Laukmanis, E., Horny, R., Wetjen, D., Manske, T., Schmidt-Stein, F., Töpker, J., Horn, S., 2018. Interaction between carbon fibers and polymer sizing: influence of fiber surface Chemistry and sizing reactivity. *Appl. Surf. Sci.* 439, 305–312. <https://doi.org/10.1016/j.apsusc.2017.12.251>.
- Morillo, J., Usero, J., Rosado, D., El Bakouri, H., Riza, A., Bernaola, F.-J., 2014. Comparative study of brine management technologies for desalination plants. *Desalination* 336, 32–49. <https://doi.org/10.1016/j.desal.2013.12.038>.
- Murthy, N.S., 1991. Metastable crystalline phases in nylon 6. *Polym. Commun.* 32.
- Oliveux, G., Dandy, L.O., Leeke, G.A., 2015. Current status of recycling of fibre reinforced polymers: review of technologies, reuse and resulting properties. *Prog. Mater. Sci.* 72, 61–99. <https://doi.org/10.1016/j.pmatsci.2015.01.004>.
- OSPAR Commission - Scoping Study on Best Practices for the Design and Recycling of Fishing Gear as a Means to Reduce the Quantities of Fishing Gear Found as Marine Litter in the North-East Atlantic Available online: <https://www.ospar.org/documents?v=42718>.
- Ozgur, C., Senel, K., Aykut-Senel, B., Bekaroglu, S.S.K., 2023. Treatment of net washing wastewater by fenton process. *Glob. Nest J.* 25, 156–162. <https://doi.org/10.30955/gnj.005088>.
- Parris, T.M., Kates, R.W., 2003. Characterising and measuring sustainable development. *Annu. Rev. Environ. Resour.* 28, 559–586. <https://doi.org/10.1146/annurev.energy.28.050302.105551>.
- Pasciucco, F., Pecorini, I., Di Gregorio, S., Pilato, F., Iannelli, R., 2021. Recovery strategies of contaminated marine sediments: a life cycle assessment. *Sustainability* 13, 8520. <https://doi.org/10.3390/su13158520>.
- Pasciucco, F., Pecorini, I., Iannelli, R., 2023a. Centralization of wastewater treatment in a tourist area: a comparative LCA considering the impact of seasonal changes. *Sci. Total Environ.* 897, 165390. <https://doi.org/10.1016/j.scitotenv.2023.165390>.
- Pasciucco, F., Francini, G., Pecorini, I., Baccioli, A., Lombardi, L., Ferrari, L., 2023b. Valorization of biogas from the anaerobic Co-treatment of sewage sludge and organic waste: life cycle assessment and life cycle costing of different recovery strategies. *J. Clean. Prod.* 401, 136762. <https://doi.org/10.1016/j.jclepro.2023.136762>.
- Peng, L., Fu, D., Qi, H., Lan, C.Q., Yu, H., Ge, C., 2020. Micro- and nano-plastics in marine environment: source, distribution and threats — a review. *Sci. Total Environ.* 698, 134254. <https://doi.org/10.1016/j.scitotenv.2019.134254>.
- Plastic Europe: Plastics - The Facts Available online: <https://plasticseurope.org/knowledge-hub/plastics-the-facts-2022/>.
- Qaidi, S.M.A., Mohammed, A.S., Ahmed, H.U., Faraj, R.H., Emad, W., Tayeh, B.A., Althoey, F., Zaid, O., Sor, N.H., 2022. Rubberized geopolymer composites: a comprehensive review. *Ceram. Int.* 48, 24234–24259. <https://doi.org/10.1016/j.ceramint.2022.06.123>.
- Qasim, M., Badrelzaman, M., Darwish, N.N., Darwish, N.A., Hilal, N., 2019. Reverse osmosis desalination: a state-of-the-art review. *Desalination* 459, 59–104. <https://doi.org/10.1016/j.desal.2019.02.008>.
- Romani, A., Caba, S., Suriano, R., Levi, M., 2023. Recycling glass and carbon fibers for reusable components in the automotive sector through additive manufacturing. *Appl. Sci.* 13, 5848. <https://doi.org/10.3390/app13105848>.
- Romero-Gómez, M.I., Silva, R.V., Flores-Colen, I., Rubio-de-Hita, P., 2023. Mechanical performance of waste fishing net fibre-reinforced gypsum composites. *Construct. Build. Mater.* 387, 131675. <https://doi.org/10.1016/j.conbuildmat.2023.131675>.
- Rossi, D., Cappello, M., Filippi, S., Bartoli, M., Malucelli, G., Cinelli, P., Seggiani, M., 2024. Polyamide 6 recycled fishing nets modified with biochar fillers: an effort toward sustainability and circularity. *Mater. Today Commun.* 41, 110650. <https://doi.org/10.1016/j.mtcomm.2024.110650>.
- Salas, A., Berrio, M.E., Martel, S., Díaz-Gómez, A., Palacio, D.A., Tuninetti, V., Medina, C., Meléndez, M.F., 2023. Towards recycling of waste carbon fiber: strength, morphology and structural features of recovered carbon fibers. *Waste Manag.* 165, 59–69. <https://doi.org/10.1016/j.wasman.2023.04.017>.
- Sandak, A., Sandak, J., Modzelewska, I., 2019. Manufacturing fit-for-purpose paper packaging containers with controlled biodegradation rate by optimizing addition of natural fillers. *Cellulose* 26, 2673–2688. <https://doi.org/10.1007/s10570-018-02235-6>.
- Santolini, E., Bovo, M., Barbaresi, A., Torreggiani, D., Tassinari, P., 2023. LCA of virgin and recycled materials to assess the sustainability of paved surfaces in agricultural environment. *J. Clean. Prod.* 393, 136291. <https://doi.org/10.1016/j.jclepro.2023.136291>.
- Schwarz, S., Höftberger, T., Burgstaller, C., Hackl, A., Schwarzingner, C., 2020. Pyrolytic recycling of carbon fibers from prepregs and their use in polyamide composites. *Open J. Compos. Mater.* 10, 92–105. <https://doi.org/10.4236/ojcm.2020.104007>.
- Single-Use Plastic (SUP) Directive EU 2019/904 Available online: <https://eur-lex.europa.eu/eli/dir/2019/904/oj>.
- Srinivasan, G., Muthukumar, P., 2021. A review on solar greenhouse dryer: design, thermal modelling, energy, economic and environmental aspects. *Sol. Energy* 229, 3–21. <https://doi.org/10.1016/j.solener.2021.04.058>.
- Study on Circular Design of the Fishing Gear for Reduction of Environmental Impacts: EASME/EMFF/2018/011 Specific Contract No. 1 (Issue 1) Available online: <http://www.europa.eu>.
- Thirugnanasambandham, K., Sivakumar, V., Shine, K., 2016. Optimization of reverse osmosis treatment process to reuse the distillery wastewater using taguchi design. *Desalination Water Treat.* 57, 24222–24230. <https://doi.org/10.1080/19443994.2016.1141323>.
- Tiwari, S., Bijwe, J., 2014. Surface treatment of carbon fibers - a review. *Procedia Technol.* 14, 505–512. <https://doi.org/10.1016/j.protcy.2014.08.064>.
- Toray Composite Materials America, Inc. Available online: <https://www.toraycma.com/page.php?id=662>.
- Unis Ahmed, H., Mahmood, L.J., Muhammad, M.A., Faraj, R.H., Qaidi, S.M.A., Hamah Sor, N., Mohammed, A.S., Mohammed, A.A., 2022. Geopolymer concrete as a cleaner construction material: an overview on materials and structural performances. *Clean. Mater.* 5, 100111. <https://doi.org/10.1016/j.clema.2022.100111>.
- Valente, M., Sambucci, M., Rossitti, I., Abruzzese, S., Sergi, C., Sarasini, F., Tirillò, J., 2023. Carbon-fiber-recycling strategies: a secondary waste stream used for PA6,6 thermoplastic composite applications. *Materials* 16. <https://doi.org/10.3390/ma16155436>.
- Vilaplana, F., Karlsson, S., 2008. Quality concepts for the improved use of recycled polymeric materials: a review. *Macromol. Mater. Eng.* 293, 274–297. <https://doi.org/10.1002/mame.200700393>.
- Wang, S., Yao, L., Jin, J., Li, G., Yang, S., 2020. Effect of air oxidation treatment on interfacial properties of carbon fibers. *Mater. Sci. Forum* 993 MSF, 695–700. <http://doi.org/10.4028/www.scientific.net/MSF.993.695>.
- Wei, Y., Hadigheh, S.A., 2023. Development of an innovative hybrid thermo-chemical recycling method for CFRP waste recovery. *Composites, Part B* 260, 110786. <https://doi.org/10.1016/j.compositesb.2023.110786>.
- Wei, Y., Hadigheh, S.A., 2024. Materials today sustainability enhancing carbon fibre recovery through optimised thermal recycling: kinetic analysis and operational parameter investigation. *Mater. Today Sustain.* 25, 100661. <https://doi.org/10.1016/j.mtsust.2023.100661>.
- Xiao, C., Liu, S., Gong, Y., Liu, Y., He, M., Yu, J., 2023. Reinforcement of polyamide 6 with carbon fiber surface modified by a polar cross-linked network interfacial phase. *J. Mater. Res. Technol.* 24, 362–375. <https://doi.org/10.1016/j.jmrt.2023.03.018>.
- You, J., Jee, S.M., Lee, Y.M., Lee, S.S., Park, M., Kim, T.A., Park, J.H., 2021. Carbon fiber-reinforced polyamide composites with efficient stress transfer via plasma-assisted mechanochemistry. *Compos. Part C Open Access* 6, 100209. <https://doi.org/10.1016/j.jcomc.2021.100209>.
- Zhang, Yanzhu, Zhang, Yi, Liu, Siwei, Huang, Aiping, Zhenguang, Chi, Jiarui Xu, J.E., 2011. Phase stability and melting behavior of the a and c phases of nylon 6. *J. Appl. Polym. Sci.* 120, 1885–1891. <https://doi.org/10.1002/app.33047>.
- Zhang, J., Chevali, V.S., Wang, H., Wang, C.H., 2020. Current status of carbon fibre and carbon fiber composites recycling. *Composites, Part B* 193, 108053. <https://doi.org/10.1016/j.compositesb.2020.108053>.
- Zheng, H., Zhang, W., Li, B., Zhu, J., Wang, C., Song, G., Wu, G., Yang, X., Huang, Y., Ma, L., 2022. Recent advances of interphases in carbon fiber-reinforced polymer composites: a review. *Composites, Part B* 233, 109639. <https://doi.org/10.1016/j.compositesb.2022.109639>.